AN INTERFEROMETRIC INVESTIGATION OF THE QUADRATIC ELECTRO-OPTIC EFFECT IN KDP

by

Mark Julian Gunning

Submitted in partial fulfilment of
the requirements for the degree of
Master of Science
in the Department of Physics,
University of Natal

Pietermaritzburg

Febuary 1995

ABSTRACT

In this research the magnitude and sign of the quadratic electro-optic coefficients g_{xxxx}, g_{yyxx}, and g_{zzxx} of a crystal of potassium dihydrogen phosphate (KDP) have been determined by means of a Michelson interferometer.

The first chapter introduces an eigenvalue multipole approach which is used in this thesis to account for the quadratic electro-optic effect in KDP. By way of justifying the theoretical approach adopted, examples are given of other electromagnetic phenomena which have been explained in terms of multipole contributions. The more usual index ellipsoid approach for describing electro-optic effects is presented together with commonly used procedures for solving for the principal axes of refraction and also for the orientation of the index ellipsoid in the presence of an applied field. Mention is made of the practical applications of electro-optic effects, for which KDP is used extensively, following which the electro-optic properties of KDP are discussed and analyzed. For the most part, previous measurements of the quadratic electro-optic effect involve the use of static and dynamic polarimetric techniques. These methods of measurements are discussed and a motivation for repeating the investigation by interferometric means is given.

In the second chapter an eigenvalue theory of light propagation is presented, within the electric dipole approximation, to describe light propagation in a non-absorbing crystal belonging to the symmetry point group of KDP, namely $\bar{4}2m$, to which a low-frequency electric field is applied. In particular, the applied field is considered to act along the

crystallographic x-axis and the direction of light propagation is taken, in turn, to be along the crystallographic y- and z-axes, the last being the axis of highest symmetry. For these configurations expressions are derived for the field-induced birefringence in KDP proportional to the square of the applied field.

An explanation of the phase-compensation method adopted for the measurement of the quadratic electro-optic coefficients of KDP is presented in the third chapter. This is followed by a detailed description of the experimental arrangement and the derivation of expressions for the induced path length changes in the two arms of the interferometer in terms of the field-induced properties of the KDP crystal and the piezoelectric reference plate. An account of the signal detection and lock-in technique is also presented.

The fourth chapter presents the results determined in the present research project, by means of the phase-compensation method, for the various light propagation and field configurations used. The contributions to the observed effect due to various physical mechanisms present in the experimental system, not accounted for in the theoretical approach, are discussed. Results obtained in this research are then discussed in the light of previous results, and in the context of a bond-polarizability model.

The thesis concludes with Chapter Five in which a brief summary is presented of the work undertaken, and an outline given of future research, to which the modulation interferometer developed for the KDP project may be applied.

DECLARATION

I declare that this work is a result of my own research, except where specifically indicated to the contrary, and has not been submitted for any other degree or examination to any other university.

Signed Mark Cumming Date 8/02/95

ACKNOWLEDGEMENTS

I wish to express my most sincere thanks to the following people:

Prof. R.E. Raab, for his unfailing interest, guidance, and encouragement in the supervision of this research, and for generous financial support;

Prof. C. Graham for his supervision of, and assistance with, the experimental work;

Dr. W. Kucharczyk for sharing his knowledge in the experimental field and for many helpful discussions;

Mr. A. Hill and Mr. J. Wilsenach of the Physics Department Workshop for the fabrication of many parts of the experimental apparatus;

Mr. N.A. Cullis and Mr. G. Dewar of the Electronics Workshop for their construction and willing assistance with various electronic elements used in the research;

the Foundation for Research Development for a Master's Bursary;

and my family for their continued support and encouragement.

LIST OF CONTENTS

CHAPTER ONE

REVIEW

1.1 INTRODUCTION

Historically, the term electro-optic effect was first used to describe a linear birefringence induced in a substance when a uniform electric field is applied to it. Although the scope has since broadened to include all effects induced by an electric field, whether uniform or not, the original meaning is implied when used in this thesis.

Kerr (1875) was the first to discover the existence of such an effect when he observed a birefringence induced by, and proportional to the square of, an electric field applied at right angles to the light path through a non-conducting liquid, such as carbon disulphide, and glass. This was followed some years later by the observation by Röntgen and Kundt in crystalline quartz of a birefringence linear in the field, when this field was applied perpendicular to the light path. Further investigations by Pockels of the linear electro-optic effect in crystals of quartz, tourmaline, potassium chlorate, and Rochelle salt revealed that it was independent of piezoelectrically-induced strain (Pockels 1906).

Symmetry constraints restrict the existence of the Pockels effect, that is the linear electro-optic effect, to only non-centrosymmetric media, whereas the Kerr effect, or quadratic electro-optic effect, exists in media of any symmetry. The Kerr effect, being considerably smaller than the Pockels effect, is usually neglected when the linear effect is present.

1.1.1 Theoretical treatment of the electro-optic effect

In order to explain fully the electro-optic effect in crystals, a sound macroscopic theory is needed. Previously, an eigenvalue multipole approach by Graham & Raab (1990) proved successful in explaining the linear birefringence in cubic crystals when the theory made allowance for induced electric octopoles and magnetic quadrupoles. In this approach multipole contributions of comparable magnitude induced by the electric and magnetic light-wave fields, and certain of their space and time derivatives, are consistently allowed for.

Multipole contributions beyond that of the electric dipole have, in the past, been invoked to explain a variety of electromagnetic effects, both natural and field-induced. An explanation was given by Born (1918) of optical activity in a field-free fluid, in which a magnetic dipole contribution was implicit. Even earlier in 1882, Gibbs showed that the optical activity in a fluid could be accounted for by the interaction of the field gradient of a light wave with a molecule. This is essentially an electric quadrupole interaction. However, it was not until 1969 that the comparable magnitudes of electric quadrupole and magnetic dipole contributions were allowed for in a theory of optical activity of aligned molecules (Nakano & Kimura). This was followed by a theory given by Buckingham and Dunn (1971) of the same effect and with the same conclusions but with the important addition that the observed effect was shown to be independent of the choice of origin used in the specification of the displacement vector $\underset{\sim}{r}$, which enters multipole moment definitions.

To explain the differential scattering of left and right circularly polarized light, Barron and Buckingham (1971) included contributions of

electric quadrupoles and magnetic dipoles. Later, electric octopole and magnetic quadrupole contributions were used to derive other differential light scattering expressions in a fluid (de Figueiredo & Raab 1981), as well as being shown to be responsible for Jones birefringence in certain non-magnetic crystals (Graham & Raab 1983; Graham & Raab 1994).

Then in 1990 a propagation equation, essentially an eigenvalue equation, to this latter multipole order was developed (Graham & Raab) to explain the very small linear birefringence observed in certain cubic crystals. Still to this order an explicit eigenvalue equation has recently been applied to all 32 non-magnetic point group symmetries of crystals to predict the various types of birefringence, and the responsible multipole polarizability tensors, which would occur for propagation along each of the three crystallographic axes (Graham & Raab 1994).

The theory presented in Chapter Two is based on the eigenvalue equation approach for light propagation of Graham and Raab (1990). It will be evident that the quadratic electro-optic effect in crystalline potassium dihydrogen phosphate (KDP) can be explained fully within the electric dipole approximation, where multipole contributions to the order of electric dipole are consistently allowed for. This eigenvalue approach allows us to derive an equation in terms of the crystal property tensors describing light propagation through a KDP crystal to which a low-frequency electric field is applied. Consequently, the induced birefringence in KDP which is proportional to the square of the applied field may be evaluated.

Other approaches to the theory of the electro-optic effect usually involve describing the birefringence of a crystal in terms of an index ellipsoid,

or optical indicatrix. This method, which yields equivalent results to those of the eigenvalue approach in the electric dipole approximations, is used extensively in textbooks dealing with optical properties of crystals, such as those by Born and Wolf (1980), Yariv and Yeh (1984), and Nye (1985).

Within the electric dipole approximation the field vector $\underset{\sim}{D}$ in the presence of light wave fields $\underset{\sim}{\mathcal{E}}$ and $\underset{\sim}{\mathcal{B}}$ may be written as

$$D_\alpha = \varepsilon_o \mathcal{E}_\alpha + P_\alpha \,, \tag{1.1}$$

where P_α is the electric dipole moment density that may be expressed as

$$P_\alpha = \alpha_{\alpha\beta} \mathcal{E}_\beta \,. \tag{1.2}$$

It is possible to rewrite eq. (1.1) in the following form

$$D_\alpha = \varepsilon_{\alpha\beta} \mathcal{E}_\beta \,, \tag{1.3}$$

where $\varepsilon_{\alpha\beta}$, referred to as the dielectric tensor, is defined as

$$\varepsilon_{\alpha\beta} = \varepsilon_o \left(\delta_{\alpha\beta} + \frac{1}{\varepsilon_o} \alpha_{\alpha\beta} \right) \,. \tag{1.4}$$

The expression for the energy density for a polarized anisotropic medium is well known to be (Born & Wolf 1980)

$$U = \frac{1}{2} \underset{\sim}{E} . \underset{\sim}{D} \,. \tag{1.5}$$

By means of eq. (1.3) this density may be expressed as

$$U = \frac{1}{2} \mathcal{E}_\alpha \varepsilon_{\alpha\beta} \mathcal{E}_\beta \,. \tag{1.6}$$

If one chooses principal dielectric axes such that $\alpha_{\alpha\beta}$ has non-zero components only of ε_{xx}, ε_{yy}, and ε_{zz}, then it follows that

$$U = \frac{1}{2} \mathcal{E}_x^2 \varepsilon_{xx} + \frac{1}{2} \mathcal{E}_y^2 \varepsilon_{yy} + \frac{1}{2} \mathcal{E}_z^2 \varepsilon_{zz} \tag{1.7}$$

or

$$U = \frac{D_x^2}{2\varepsilon_{xx}} + \frac{D_y^2}{2\varepsilon_{yy}} + \frac{D_z^2}{2\varepsilon_{zz}} \,. \tag{1.8}$$

Replacing $D_x/\sqrt{2\varepsilon_o U}$, $D_y/\sqrt{2\varepsilon_o U}$, and $D_z/\sqrt{2\varepsilon_o U}$ respectively with a set of Cartesian coordinates x, y, and z, and defining the refractive index in

terms of the dielectric tensor as $n_i^2 \equiv \varepsilon_{ii}/\varepsilon_o$, where $i = x, y, z$, then one may rewrite eq. (1.8) as (see, for example, Yariv & Yeh 1984)

$$\frac{x^2}{n_x^2} + \frac{y^2}{n_y^2} + \frac{z^2}{n_z^2} = 1 \ . \tag{1.9}$$

The above equation is referred to as the index ellipsoid of wave normals, in the principal coordinate system, where the origin O of the Cartesian axes is located at the centre of the ellipsoid and the axes are oriented to coincide with the principal axes of the ellipsoid. In this equation n_i is the refractive index for a monochromatic wave propagating through the medium linearly polarized parallel to the i^{th} axis. An ellipse formed by the intersection of a plane through O with the ellipsoid has principal axes which coincide with the directions of the electric induction vectors of two light waves propagating normal to the plane, and the lengths of the axes are the inverse squares of the refractive indices of these waves.

In previous work (see, for example, Kaminow 1974) an impermeability tensor is defined in terms of the dielectric tensor as

$$\eta_{\alpha\beta} = \frac{\varepsilon_o}{\varepsilon_{\alpha\beta}} \ , \tag{1.10}$$

where this tensor is intended to express $\underset{\sim}{\mathcal{E}}$ in terms of $\underset{\sim}{D}$ by means of the inverse of $\varepsilon_{\alpha\beta}$ such that

$$\mathcal{E}_\alpha = \varepsilon_o^{-1} \eta_{\alpha\beta} D_\beta \ . \tag{1.11}$$

For a principal coordinate system eq. (1.8) may be rewritten in terms of the impermeability tensor as

$$U = \eta_{xx}\frac{D_x^2}{2\varepsilon_o} + \eta_{yy}\frac{D_y^2}{2\varepsilon_o} + \eta_{zz}\frac{D_z^2}{2\varepsilon_o} \ . \tag{1.12}$$

This equation yields an expression equivalent to that of the index ellipsoid which may be written as

$$\eta_{xx}x^2 + \eta_{yy}y^2 + \eta_{zz}z^2 = 1 \ . \qquad (1.13)$$

Accordingly, changes in the shape, size, and orientation of the index ellipsoid brought about by the electro-optically-induced change in refractive index may be expressed in terms of changes to the impermeability tensor.

Pockels (1906) provided the first general treatment of the electro-optic effect. He derived the number and form of the relevant constants expected for the different crystal symmetry classes, where these numerical constants may be considered small corrections necessary to be applied to the index ellipsoid constants when an electric field is applied to the crystal. The constants that Pockels introduced were defined in terms of the electrical polarization, but were later redefined instead in terms of electric field (see, for example, Kaminow 1974). Expressing these electro-optic constants in terms of the electric field-induced changes to the impermeability tensor one may write:

$$\eta_{\alpha\beta}(\underset{\sim}{E}) - \eta_{\alpha\beta}(0) \equiv \Delta\eta_{\alpha\beta} = r_{\alpha\beta\gamma}E_\gamma + g_{\alpha\beta\gamma\delta}E_\gamma E_\delta + \ldots \ , \qquad (1.14)$$

where only terms linear and quadratic in the applied field $\underset{\sim}{E}$ have been retained. The coefficients $r_{\alpha\beta\gamma}$ and $g_{\alpha\beta\gamma\delta}$ are respectively the linear (or Pockels) and quadratic (or Kerr) electro-optic coefficients and are related directly to the structure and type of crystal under consideration.

The electro-optically-induced changes to the index ellipsoid due to the presence of an applied electric field may be used to obtain solutions to the eigenvalue problem of crystal optics. Procedures for solving for the principal indices of refraction and the orientation of the index ellipsoid, in the presence of an applied electric field, are discussed in a number of advanced optics textbooks and have recently been reviewed in an article by

Maldonado and Gaylord (1988).

The more usual approach, which is outlined by Nye (1985), involves solving a 3x3 determinantal equation, which is really a secular equation, from which the eigenvalues of the impermeability tensor may be found, and consequently the lengths and directions of the index ellipsoid determined. Another technique (see, for example, Born and Wolf 1980) involves a method of Lagrange multipliers in which a secular equation is again utilized from which the permitted directions of vibrations of the electric displacement vector $\underset{\sim}{D}$ are determined for a given path of phase propagation. A Richardson purification process (Hartree 1952) may also be used, where the eigenvectors of wave propagation are determined on the basis of successive approximations for the eigenvalues. Other approaches have involved a Mohr circle construction technique (Nye 1985), similarity transformation methods, and more recently a Jacobi matrix method (Maldonado & Gaylord 1988).

In the past, a number of attempts have been made to relate the electro-optic effect observed in crystals to other similar effects, and also to understand the mechanism of the effect in terms of various models.

Most of the earlier theoretical approaches were limited to the case of diatomic molecules. Theories have also been attempted on ionic crystals. For example, to obtain a non-linear equation for the polarization of a zinc-blende-type ionic crystal, Kelly (1966) used a generalized theory describing the dielectric properties of ionic crystals. From this result he was able to obtain an expression for the linear electro-optic coefficient for these crystals and calculate results for the linear coefficients of ZnS

and CuCl, which were in satisfactory agreement with experiment. Later, using an electrostatic point-charge model and dielectric theory, Flytzanis (1969, 1971) calculated electro-optic coefficients of various diatomic crystals.

Fowler and Madden (1984) performed *ab initio* cluster-type calculations, within a multibody perturbation scheme, of the hyperpolarizabilities of LiF and LiCl crystals, where the low-frequency electro-optic coefficients may be related to the static hyperpolarizabilities (Kaminow 1974). The values obtained were in good agreement with those achieved experimentally from three-wave-mixing and third-harmonic generation experiments.

Models for media with more general structures have also been proposed. Shih and Yariv (1980, 1982) presented a simple model in terms of bond properties to describe linear electro-optic effects in crystals of various structures and constituents. This approach has since been extended to the case of the quadratic electro-optic effect in LiF and KDP (Kucharczyk 1987, 1992) and will be discussed further in Section 4.7, where results obtained in this research are analyzed.

Other approaches have included: an energy-band picture (DiDomenico & Wemple 1969), a relation between Raman-scattering efficiencies and electro-optic coefficients measured at radio frequencies (Kaminow 1967), two-oscillator models (Barker & Loudon 1972), a local-density-approximation scheme to compute the static electronic hyperpolarizability for the alkali halide crystals (Johnson *et al.* 1987), and an application of perturbation theory to the wave equation (Nelson 1975). An estimation of the quadratic electro-optic effect in KDP was made by Jamroz and Karniewicz (1979) based

on an anharmonic oscillator model.

1.1.2 Practical applications of electro-optic effects

In the past a large amount of experimental work has been done in the field of the electro-optical properties of materials. This interest stems from the electro-optic effects of these crystals being utilized in a wide range of applications in modern optical technology.

By means of the electro-optic effect it is possible to control the phase and intensity of optical radiation. A common application of the electro-optic effect is in light modulators which offer the possibility of high speed and accurately controlled manipulation of a laser beam or in controlling the signal retardation. Moving mechanical parts which would otherwise have to be used do not allow modulation at the required frequencies, usually reaching up to the gigahertz range, due to their inertia. An ever-increasing number of appliances make use of this optical modulation. These range from optical beam deflectors and spectral tunable filters to the impression of information into optical beams for communication purposes. Electro-optic devices are also used in analogue and digital signal processing and optical computing; as well as in the development of sensors to detect humidity, temperature, and electric signals at radio frequencies.

The Kerr effect is utilized extensively in Q-switches in pulsed laser systems, and also in optical modulators and Kerr shutters, where the quadratic effect provides the advantage of effective modulation response at higher frequencies.

It may be concluded that the precise determination of the magnitude and sign of electro-optic coefficients is important not only for the optimization and design of electro-optic devices which are based on the effects, but also to acquire an insight into the physics of these and related phenomena.

1.2 A REVIEW OF POTASSIUM DIHYDROGEN PHOSPHATE

The particular electro-optic crystal under consideration in this research is crystalline potassium dihydrogen phosphate (KH_2PO_4). Better known as KDP, its notable non-linear properties place it amongst the most widely known of the electro-optic crystals. It exhibits a large linear electro-optic effect which is utilized extensively in electro-optic devices.

1.2.1 General properties of KDP

Due to the large interest shown in the practical application of KDP crystals, the properties of this compound have been investigated thoroughly over the past 50 years. A review of the general properties of KDP follows.

At room temperature KDP crystals are paraelectric and belong to the tetragonal symmetry point group $\bar{4}2m$. On cooling below about 123 K KDP undergoes a ferroelectric phase transition and at these lower temperatures the crystal symmetry is orthorhombic mm2. In both phases the crystals are piezoelectric. KDP is known to be transparent for wavelengths as short as 0.2 μm and up to 2.0 μm, and over this range the index of refraction and electro-optic coefficients are known to be almost constant (Shih & Yariv 1982).

KDP crystals, grown at room temperature from water solution, are generally free from strains often found in crystals grown at higher temperatures, and tend to have good to excellent optical properties. It is possible to obtain commercially relatively large, good quality crystals which, though hygroscopic and fragile, may be cut and polished without difficulty. The resistivity of a KDP crystal is typically 10^{12} Ωm; this high resistance means that during experimentation at high electric field strengths there is no appreciable flow of current which could possibly lead to excessive heating of the sample.

1.2.2 Electro-optic effects in KDP

Crystals of the KDP-type family lack a centre of inversion and consequently they may simultaneously exhibit both linear and quadratic electro-optic effects, if permitted by symmetry considerations for the particular field and light directions chosen. In the following research, symmetry conditions are considered for which the linear electro-optic effect, and other odd-order effects, are eliminated. Consequently the quadratic electro-optic effect becomes the leading term.

Due to symmetry constraints (Birss 1966) and intrinsic symmetry, only two independent components of the linear electro-optic tensor of KDP exist (see Section 2.2). These linear coefficients have been investigated thoroughly by several authors employing a number of transmission experimental techniques, and are found to be $r_{xyz} = -10.5 \times 10^{-12}$ mV^{-1} and $r_{yzx} = r_{xzy} = -8.8 \times 10^{-12}$ mV^{-1} (Landolt-Börnstein 1979). The quadratic electro-optic effects in KDP are described by seven independent components g_{xxxx}, g_{zzzz}, g_{xxyy}, g_{xxzz}, g_{zzxx}, g_{xyxy}, and g_{xzxz} (see Section 2.2). In comparison with the linear effect, the quadratic effect in KDP is small and consequently

difficult to measure. As a result there is a large spread in the results obtained experimentally for these coefficients. With one notable exception (Grib *et al.* 1975), the methods for measuring the quadratic effect in KDP have employed polarimetric techniques.

Table 1.1 reflects the large disagreement found in experimental results obtained thus far. Indeed, it has been noted (Górski & Kucharczyk 1987, 1990) that the results obtained for KDP-group crystals for both the quadratic and fourth-order electro-optic coefficients by means of the dynamic and static polarimetric techniques differ by orders of magnitude. The range of these values cannot be explained in terms of the dispersion of the electro-optic coefficients or their temperature dependence, since the coefficients are known to be almost independent of the optical wavelength for the transparent region of the crystal, and the results quoted were all obtained at room temperature.

The fact that the measured values for the quadratic electro-optic coefficients of KDP range over two orders of magnitude makes the remeasurement of these coefficients by a different technique important.

1.3 THE MEASUREMENT OF ELECTRO-OPTIC EFFECTS

In the polarimetric technique the electro-optic crystal is placed between a polarizer and analyzer, which are not necessarily crossed, and the intensity transmitted by the system is measured relative to that incident on it. The field-induced birefringence has been measured in this way in the past (see, for example, Górski & Kucharczyk 1987). An arrangement typifying those used in polarimetric determinations of electro-optic coefficients is shown in Figure 1.1.

The relative light intensity transmitted by such an optical arrangement is given by (Born & Wolf 1980)

$$I/I_o = \cos^2(\chi) - \sin(2\alpha)\sin(2[\alpha-\chi])\sin^2(\Delta\Gamma/2) \quad . \qquad (1.15)$$

In the above equation I_o is the light intensity of the incident beam, α is the angle between the transmission axis of the polarizer and the principal axis of the elliptical cross-section of the index ellipsoid, χ is the angle between the transmission axes of the polarizer and analyzer, and $\Delta\Gamma$ is the phase shift between the ordinary and extraordinary rays after passing through the retardance plate and the crystal of length l. An expression for the phase shift may be written as

$$\Delta\Gamma = \Gamma_o + \frac{2\pi l \Delta n}{\lambda} \quad , \qquad (1.16)$$

where Γ_o is the phase shift introduced by the retardance plate, Δn is the field-induced birefringence, and λ is the wavelength of the propagating light wave. For specific experimental arrangements, in which the polarizer and analyzer are usually either parallel or crossed, the expression given in eq. (1.15) for the relative light intensity is simplified.

It follows that when an electric field is applied to the crystal, measurements of the change in intensity may be related to the field-induced birefringence Δn, where, for a particular configuration, Δn is related to the relevant electro-optic coefficients of the crystal and the applied field. Essentially, polarimetric techniques involve measuring the change in intensity of the transmitted light as a function of the field applied to the crystal. From this relationship, which has the form of eq. (1.15), and from an expression for the field-induced birefringence for the particular applied field and light propagation directions being considered, values for the crystal's electro-optic coefficients in question may be found by

extrapolation.

In the static polarimetric technique a dc voltage is applied across the crystal sample. Electro-optic coefficients of the crystal are then determined from the change in intensity as a function of the applied voltage. Dynamic polarimetric methods involve the application of a sinusoidal electric field of low frequency ω to the sample. This alternating voltage results in a modulation of the transmitted light intensity. It is therefore possible to perform a harmonic analysis of the transmitted signal by means of, for example, a lock-in amplifier. This method of detection affords a sensitivity unavailable in static measurement techniques. In the dynamic polarimetric method, values of the quadratic electro-optic coefficients are obtained from the dependence of the modulation index $I^{2\omega}/I_o$ on the square of the applied field, where $I^{2\omega}$ is the intensity of the second harmonic of the modulated low-frequency field (Górski & Kucharczyk 1987).

The experimental determination of electro-optic effects is not restricted to polarimetric techniques and various interferometric approaches have also been utilized. This latter method offers a simple, yet sensitive, means of optical study.

In the interferometric technique the sample to be investigated is placed in an arm of the interferometer. As the electro-optic effect leads to a birefringence induced in the sample by an electric field applied to it, a light beam propagating through the sample undergoes a shift in phase. This phase shift leads to a change in intensity of the interference pattern formed by the beams on recombining after having traversed the arms of the

interferometer. Measuring this intensity change allows the sample's electro-optic effect to be determined.

Zook *et al.* (1967) made use of a modified Michelson interferometer in order to determine the sign, magnitude, and temperature dependence of the linear electro-optic effect in $LiNbO_3$ crystals. Their experimental procedure consisted of measuring the modulated phase shift induced in the sample against that established by the sine-wave vibration of a reference mirror in the other arm of the interferometer. Adopting a different approach Onuki *et al.* (1972) used a Mach-Zehnder interferometer to determine the linear electro-optic coefficients of KDP, $LiNbO_3$, and a number of other compounds. Their method was based on compensating for the shift in phase induced in the sample by that induced in a reference material of known electro-optic response. A Mach-Zehnder interferometric approach has also been used to study electro-optic effects in thin films of $LiNbO_3$ (Fukunishi *et al.* 1974).

When applied to electro-optic measurements the interferometric method has several intrinsic advantages over the traditional polarimetric techniques. As well as being of comparable sensitivity, which is invaluable in measuring small electro-optic effects, the interferometric approach allows the changes in refractive indices along the principal axes of the crystal to be determined independently, along with the sign which enables individual electro-optic coefficients to be evaluated. The polarimetric method allows the possibility of determining only the absolute value of relative coefficients and not the magnitude and sign of each coefficient separately. It is important to know the signs of the coefficients when relating the quadratic electro-optic effect to other non-linear phenomena

and in applying theoretical models to non-linear susceptibilities.

The method of measurement adopted in this investigation uses a vibrating-mirror Michelson interferometer to perform simple yet highly sensitive compensation measurements to determine the quadratic electro-optic coefficients g_{xxxx}, g_{yyxx}, and g_{zzxx} of KDP. This experimental method is detailed in Chapter Three.

CHAPTER TWO

THE QUADRATIC ELECTRO-OPTIC EFFECT IN KDP

2.1 AN EIGENVALUE EQUATION OF LIGHT PROPAGATION

By means of the two Maxwell equations

$$\nabla \times \underset{\sim}{E} = -\dot{\underset{\sim}{B}} , \tag{2.1}$$

$$\nabla \times \underset{\sim}{H} = \dot{\underset{\sim}{D}} , \tag{2.2}$$

an eigenvalue equation may be derived in terms of multipole polarizability tensors, which describes the propagation of a plane monochromatic light wave through a source-free medium. In this thesis, non-magnetic crystals are considered for wavelengths far from absorption bands. As will be apparent later, the eigenvalue equation allows the two polarization eigenvectors to be determined, and expressions to be obtained for their respective refractive indices in terms of macroscopic polarizability tensors of the medium, for any direction of phase propagation of the light wave through the medium.

When using Maxwell's equations to describe a range of electromagnetic effects in matter, it is convenient to adopt the multipole approach: the $\underset{\sim}{D}$ and $\underset{\sim}{H}$ field vectors in eq. (2.2) are expanded in multipole form, taking care to include in both fields multipole contributions of comparable magnitude. The relative magnitudes of multipole contributions to a physical effect are ordered as follows (de Figueiredo & Raab 1981):

$$\text{electric dipole} \gg \begin{cases} \text{electric quadrupole} \\ \text{magnetic dipole} \end{cases} \gg \begin{cases} \text{electric octopole} \\ \text{magnetic quadrupole} \end{cases} \gg \ldots . \tag{2.3}$$

Correct forms for $\underset{\sim}{D}$ and $\underset{\sim}{H}$ in the electric octopole-magnetic quadrupole approximation are (Graham *et al.* 1992)

$$D_\alpha = \varepsilon_o \mathcal{E}_\alpha + P_\alpha - \tfrac{1}{2}\nabla_\beta Q_{\alpha\beta} + \tfrac{1}{6}\nabla_\gamma \nabla_\beta Q_{\alpha\beta\gamma} - \ldots \,, \tag{2.4}$$

$$H_\alpha = \mu_o^{-1} \mathcal{B}_\alpha - M_\alpha + \tfrac{1}{2}\nabla_\beta M_{\alpha\beta} - \ldots \,, \tag{2.5}$$

in which Greek subscripts are used to specify Cartesian components of a tensor. In eq. (2.4) P_α, $Q_{\alpha\beta}$, and $Q_{\alpha\beta\gamma}$ are respectively the electric dipole, quadrupole, and octopole moments per unit macroscopic volume, while in eq. (2.5) M_α and $M_{\alpha\beta}$ respectively are the corresponding quantities for the magnetic dipole and quadrupole moments. These multipole moment densities are the averages per unit macroscopic volume of the following moments of a charge distribution, defined by (Raab 1975)

$$\begin{aligned}
\text{electric dipole} \quad & p_\alpha = \sum q r_\alpha \,, \\
\text{electric quadrupole} \quad & q_{\alpha\beta} = \sum q r_\alpha r_\beta \,, \\
\text{electric octopole} \quad & q_{\alpha\beta\gamma} = \sum q r_\alpha r_\beta r_\gamma \,, \\
\text{magnetic dipole} \quad & m_\alpha = \sum \left(\frac{q}{2m}\right) \ell_\alpha \,, \\
\text{magnetic quadrupole} \quad & m_{\alpha\beta} = \sum \left(\frac{q}{3m}\right) (r_\beta \ell_\alpha + \ell_\alpha r_\beta) \,,
\end{aligned} \tag{2.6}$$

where q is the charge, m the mass, and $\underset{\sim}{\ell} = \underset{\sim}{r} \times \underset{\sim}{p}$ the orbital angular momentum of a particle that has a displacement $\underset{\sim}{r}$ from an arbitrary origin inside the distributions. $\sum$ denotes a summation over all its particles.

A plane light wave of angular frequency ω possesses electric and magnetic fields, $\underset{\sim}{\mathcal{E}}$ and $\underset{\sim}{\mathcal{B}}$, as well as their space variation to all orders but, due to the simple harmonic property of a monochromatic wave, only two independent time derivatives of each, which are taken as the field and its first time derivative. The fields, and their space and time derivatives, of a light wave passing through a material induce multipole moments in a macroscopic volume element. To the order of electric octopole and magnetic quadrupole their densities are given by (Buckingham 1967; de Figueiredo & Raab 1981)

$$
\begin{aligned}
P_\alpha &= \alpha_{\alpha\beta}\mathcal{E}_\beta + \tfrac{1}{\omega}\alpha'_{\alpha\beta}\dot{\mathcal{E}}_\beta + \tfrac{1}{2}a_{\alpha\beta\gamma}\nabla_\gamma\mathcal{E}_\beta + \tfrac{1}{2\omega}a'_{\alpha\beta\gamma}\nabla_\gamma\dot{\mathcal{E}}_\beta + \tfrac{1}{6}b_{\alpha\beta\gamma\delta}\nabla_\delta\nabla_\gamma\mathcal{E}_\beta \\
&\quad + \tfrac{1}{6\omega}b'_{\alpha\beta\gamma\delta}\nabla_\delta\nabla_\gamma\dot{\mathcal{E}}_\beta + \ldots + G_{\alpha\beta}\mathcal{B}_\beta + \tfrac{1}{\omega}G'_{\alpha\beta}\dot{\mathcal{B}}_\beta + \tfrac{1}{2}H_{\alpha\beta\gamma}\nabla_\gamma\mathcal{B}_\beta \\
&\quad + \tfrac{1}{2\omega}H'_{\alpha\beta\gamma}\nabla_\gamma\dot{\mathcal{B}}_\beta + \ldots , \\
Q_{\alpha\beta} &= a_{\alpha\beta\gamma}\mathcal{E}_\gamma + \tfrac{1}{\omega}a'_{\alpha\beta\gamma}\dot{\mathcal{E}}_\gamma + \tfrac{1}{2}d_{\alpha\beta\gamma\delta}\nabla_\delta\mathcal{E}_\gamma + \tfrac{1}{2\omega}d'_{\alpha\beta\gamma\delta}\nabla_\delta\dot{\mathcal{E}}_\gamma + \ldots + L_{\alpha\beta\gamma}\mathcal{B}_\gamma \\
&\quad + \tfrac{1}{\omega}L'_{\alpha\beta\gamma}\dot{\mathcal{B}}_\gamma + \ldots , \qquad (2.7) \\
Q_{\alpha\beta\gamma} &= \mathfrak{b}_{\alpha\beta\gamma\delta}\mathcal{E}_\delta + \tfrac{1}{\omega}\mathfrak{b}'_{\alpha\beta\gamma\delta}\dot{\mathcal{E}}_\delta + \ldots , \\
M_\alpha &= \mathcal{G}_{\alpha\beta}\mathcal{E}_\beta + \tfrac{1}{\omega}\mathcal{G}'_{\alpha\beta}\dot{\mathcal{E}}_\beta + \tfrac{1}{2}\mathcal{L}_{\alpha\beta\gamma}\nabla_\gamma\mathcal{E}_\beta + \tfrac{1}{2\omega}\mathcal{L}'_{\alpha\beta\gamma}\nabla_\gamma\dot{\mathcal{E}}_\beta + \ldots + \chi_{\alpha\beta}\mathcal{B}_\beta \\
&\quad + \tfrac{1}{\omega}\chi'_{\alpha\beta}\dot{\mathcal{B}}_\beta + \ldots , \\
M_{\alpha\beta} &= \mathcal{H}_{\alpha\beta\gamma}\mathcal{E}_\gamma + \tfrac{1}{\omega}\mathcal{H}'_{\alpha\beta\gamma}\dot{\mathcal{E}}_\gamma + \ldots ,
\end{aligned}
$$

where the polarizability tensors $\alpha_{\alpha\beta}$, $\alpha'_{\alpha\beta}$, $a_{\alpha\beta\gamma}$, $a'_{\alpha\beta\gamma}$, etc. are macroscopic volume properties of the medium.

In terms of the relative orders of magnitude of the multipole moments in eq. (2.3) the distortion or polarizability tensors in eqs. (2.7) fall into three groups:

$$
\begin{aligned}
&\text{electric dipole} : \quad \alpha_{\alpha\beta},\ \alpha'_{\alpha\beta}, \\
&\left.\begin{matrix}\text{electric quadrupole}\\ \text{magnetic dipole}\end{matrix}\right\} : \quad \{a_{\alpha\beta\gamma},\ a'_{\alpha\beta\gamma},\ a_{\alpha\beta\gamma},\ a'_{\alpha\beta\gamma},\ G_{\alpha\beta},\ G'_{\alpha\beta},\ \mathcal{G}_{\alpha\beta},\ \mathcal{G}'_{\alpha\beta}, \\
&\left.\begin{matrix}\text{electric octopole}\\ \text{magnetic quadrupole}\end{matrix}\right\} : \quad \begin{cases} b_{\alpha\beta\gamma\delta},\ b'_{\alpha\beta\gamma\delta},\ \mathfrak{b}_{\alpha\beta\gamma\delta},\ \mathfrak{b}'_{\alpha\beta\gamma\delta},\ d_{\alpha\beta\gamma\delta},\ d'_{\alpha\beta\gamma\delta}, \\ H_{\alpha\beta\gamma},\ H'_{\alpha\beta\gamma},\ \mathcal{H}_{\alpha\beta\gamma},\ \mathcal{H}'_{\alpha\beta\gamma},\ L_{\alpha\beta\gamma},\ L'_{\alpha\beta\gamma},\ \mathcal{L}_{\alpha\beta\gamma}, \\ \mathcal{L}'_{\alpha\beta\gamma},\ \chi_{\alpha\beta},\ \chi'_{\alpha\beta}\ . \end{cases} \qquad (2.8)
\end{aligned}
$$

This classification follows from the quantum-mechanical expressions of these tensors derived in Section 2.3. Depending on their behaviour under time and space inversion these polarizability tensors may be classified as time-invariant tensors (*i*-tensors) or time-changing tensors (*c*-tensors), and as polar or axial tensors. For non-magnetic crystals, considered in this work, *c*-tensors need not be retained as they are properties of magnetic crystals only (Birss 1966).

Previously, multipole contributions beyond that of the electric dipole have been used to explain a number of electromagnetic effects, as is mentioned in Chapter One. In this chapter the theory of the quadratic electro-optic effect in crystalline potassium dihydrogen phosphate (KDP) is presented. It will become evident that this effect may be explained within the electric dipole approximation. Accordingly, the derivation of the eigenvalue equation for describing the propagation of a light wave in a crystal, to which a uniform electric field is applied, takes into account only induced electric dipoles.

Considering $\underset{\sim}{D}$ and $\underset{\sim}{H}$ in the presence of the light-wave fields only, one may write

$$D_\alpha = \varepsilon_o \mathcal{E}_\alpha + P_\alpha \,, \tag{2.9}$$

$$H_\alpha = \mu_o^{-1} \mathcal{B}_\alpha \,, \tag{2.10}$$

where for non-magnetic crystals

$$P_\alpha = \alpha_{\alpha\beta} \mathcal{E}_\beta \,. \tag{2.11}$$

The electric field of a plane monochromatic light wave may be expressed in the complex form

$$\underset{\sim}{\mathcal{E}} = \underset{\sim}{\mathcal{E}}^{(o)} e^{-i\omega(t - n\underset{\sim}{r}.\underset{\sim}{\sigma}/c)} \,. \tag{2.12}$$

where n is the refractive index for the polarization state of amplitude $\underset{\sim}{\mathcal{E}}^{(o)}$ propagating in the direction of the unit vector $\underset{\sim}{\sigma}$ along the wavefront normal, and ω is the angular frequency of the light wave. As a result, it is possible to express $\underset{\sim}{\mathcal{B}}$ in terms of $\underset{\sim}{\mathcal{E}}$ from eq. (2.1) as

$$\underset{\sim}{\mathcal{B}} = \frac{n}{c}\left(\underset{\sim}{\sigma} \times \underset{\sim}{\mathcal{E}}\right) \,. \tag{2.13}$$

By means of eqs. (2.11) to (2.13), $\underset{\sim}{D}$ and $\underset{\sim}{H}$ in eqs. (2.9) and (2.10) may be expressed in terms of $\underset{\sim}{\mathcal{E}}$, and so therefore may eq. (2.2), namely

$$\left[n^2\sigma_\alpha\sigma_\beta - (n^2 - 1)\delta_{\alpha\beta} + \frac{1}{\varepsilon_o}\alpha_{\alpha\beta}\right]\mathcal{E}_\beta^{(o)} = 0 \ . \qquad (2.14)$$

In the above equation the phase part of $\underset{\sim}{\mathcal{E}}$, which is not necessarily zero for all space and time, has been cancelled. The propagation unit vector $\underset{\sim}{\sigma}$ of the light wave and the electric-field amplitude $\underset{\sim}{\mathcal{E}}^{(o)}$ may be specified in terms of a laboratory frame of Cartesian axes x, y, and z. As eq. (2.14) is essentially the Maxwell vector equation eq. (2.2), it is really three equations which are obtained by setting $\alpha = x, y, z$ in turn, leading to three linear homogeneous equations in the components of $\underset{\sim}{\mathcal{E}}^{(o)}$. These may be written in the matrix form as

$$\begin{bmatrix} n^2(\sigma_x^2 - 1) + 1 + \frac{1}{\varepsilon_o}\alpha_{xx} & n^2\sigma_x\sigma_y + \frac{1}{\varepsilon_o}\alpha_{xy} & n^2\sigma_x\sigma_z + \frac{1}{\varepsilon_o}\alpha_{xz} \\ n^2\sigma_y\sigma_x + \frac{1}{\varepsilon_o}\alpha_{yx} & n^2(\sigma_y^2 - 1) + 1 + \frac{1}{\varepsilon_o}\alpha_{yy} & n^2\sigma_y\sigma_z + \frac{1}{\varepsilon_o}\alpha_{yz} \\ n^2\sigma_z\sigma_x + \frac{1}{\varepsilon_o}\alpha_{zx} & n^2\sigma_z\sigma_y + \frac{1}{\varepsilon_o}\alpha_{zy} & n^2(\sigma_z^2 - 1) + 1 + \frac{1}{\varepsilon_o}\alpha_{zz} \end{bmatrix} \begin{bmatrix} \mathcal{E}_x^{(o)} \\ \mathcal{E}_y^{(o)} \\ \mathcal{E}_z^{(o)} \end{bmatrix}$$

$$= 0 \ . \qquad (2.15)$$

This equation may be re-arranged into a matrix eigenvalue form, namely

$$\begin{bmatrix} n^2(1 - \sigma_x^2) - \frac{1}{\varepsilon_o}\alpha_{xx} & -n^2\sigma_x\sigma_y - \frac{1}{\varepsilon_o}\alpha_{xy} & -n^2\sigma_x\sigma_z - \frac{1}{\varepsilon_o}\alpha_{xz} \\ -n^2\sigma_y\sigma_x - \frac{1}{\varepsilon_o}\alpha_{yx} & n^2(1 - \sigma_y^2) - \frac{1}{\varepsilon_o}\alpha_{yy} & -n^2\sigma_y\sigma_z - \frac{1}{\varepsilon_o}\alpha_{yz} \\ -n^2\sigma_z\sigma_x - \frac{1}{\varepsilon_o}\alpha_{zx} & -n^2\sigma_z\sigma_y - \frac{1}{\varepsilon_o}\alpha_{zy} & n^2(1 - \sigma_z^2) - \frac{1}{\varepsilon_o}\alpha_{zz} \end{bmatrix} \begin{bmatrix} \mathcal{E}_x^{(o)} \\ \mathcal{E}_y^{(o)} \\ \mathcal{E}_z^{(o)} \end{bmatrix} = \begin{bmatrix} \mathcal{E}_x^{(o)} \\ \mathcal{E}_y^{(o)} \\ \mathcal{E}_z^{(o)} \end{bmatrix} ,$$

(2.16)

in which the eigenvalues are unity. This value constrains the refractive index n to a certain value for each of the eigenvectors, as specified by the components of $\underset{\sim}{\mathcal{E}}^{(o)}$, which represent the polarization forms which the medium will support for propagation in the direction of $\underset{\sim}{\sigma}$.

Equation (2.14), or alternatively eq. (2.16), is the fundamental equation within the electric dipole approximation for describing light

propagation in a field-free non-magnetic medium.

Instead of solving eq. (2.16) for the polarization eigenvectors, it is simpler to approach the solution in another way. The condition that there are non-trivial solutions for the three components of $\underset{\sim}{\mathcal{E}}^{(o)}$ is that the determinant of their coefficients should vanish. Thus

$$\begin{vmatrix} n^2(\sigma_x^2 - 1) + 1 + \frac{1}{\varepsilon_o}\alpha_{xx} & n^2\sigma_x\sigma_y + \frac{1}{\varepsilon_o}\alpha_{xy} & n^2\sigma_x\sigma_z + \frac{1}{\varepsilon_o}\alpha_{xz} \\ n^2\sigma_y\sigma_x + \frac{1}{\varepsilon_o}\alpha_{yx} & n^2(\sigma_y^2 - 1) + 1 + \frac{1}{\varepsilon_o}\alpha_{yy} & n^2\sigma_y\sigma_z + \frac{1}{\varepsilon_o}\alpha_{yz} \\ n^2\sigma_z\sigma_x + \frac{1}{\varepsilon_o}\alpha_{zx} & n^2\sigma_z\sigma_y + \frac{1}{\varepsilon_o}\alpha_{zy} & n^2(\sigma_z^2 - 1) + 1 + \frac{1}{\varepsilon_o}\alpha_{zz} \end{vmatrix} = 0 \ . \qquad (2.17)$$

This is the secular equation obtained from eq. (2.15). Its solution yields the values of n associated with each of the polarization eigenvectors, which may be found in turn by substituting back each n value into the three equations contained in eq. (2.15).

2.2 AN EIGENVALUE EQUATION IN THE PRESENCE OF AN APPLIED ELECTRIC FIELD

2.2.1 General case for a non-magnetic crystal

Consider a static, or low-frequency,[1] uniform electric field $\underset{\sim}{E}$ applied to a non-magnetic crystal. Within the electric dipole approximation the expression for the polarization density induced in the medium by a monochromatic plane light wave, in the presence of this applied field, is (Buckingham & Pople 1955)

$$P_\alpha = \alpha_{\alpha\beta}\mathcal{E}_\beta + \tfrac{1}{2}\beta_{\alpha\beta\gamma}\mathcal{E}_\beta E_\gamma + \tfrac{1}{6}\gamma_{\alpha\beta\gamma\delta}\mathcal{E}_\beta E_\gamma E_\delta + \ldots \ . \qquad (2.18)$$

Alternatively, one may regard $\alpha_{\alpha\beta}$ in eq. (2.11) to be perturbed by the

---

[1] A low-frequency field is considered to have a frequency well below the lattice resonances of the medium.

applied field and write

$$P_\alpha = \alpha_{\alpha\beta}(\underset{\sim}{E})\mathcal{E}_\beta \ , \tag{2.19}$$

where $\alpha_{\alpha\beta}(\underset{\sim}{E})$ may then be Taylor-expanded in powers of $\underset{\sim}{E}$ as follows:

$$\alpha_{\alpha\beta}(\underset{\sim}{E}) = \alpha_{\alpha\beta} + \tfrac{1}{2}\beta_{\alpha\beta\gamma}E_\gamma + \tfrac{1}{6}\gamma_{\alpha\beta\gamma\delta}E_\gamma E_\delta + \ldots \ , \tag{2.20}$$

$\alpha_{\alpha\beta}$ being the polarizability, and $\beta_{\alpha\beta\gamma}$ and $\gamma_{\alpha\beta\gamma\delta}$ the first- and second-order hyperpolarizability tensors of the medium respectively. These tensors are field-free properties. In a study of the quadratic electro-optic effect it is necessary to retain only the terms linear and quadratic in the applied field as higher-order terms are considered negligible.

Thus from eqs. (2.9) to (2.11), and (2.20) when a strong uniform electric field is applied to a source-free non-magnetic medium, the expressions for $\underset{\sim}{D}$ and $\underset{\sim}{H}$ within the electric dipole approximation now become

$$D_\alpha = \varepsilon_o E_\alpha + (\varepsilon_o\delta_{\alpha\beta} + \alpha_{\alpha\beta} + \tfrac{1}{2}\beta_{\alpha\beta\gamma}E_\gamma + \tfrac{1}{6}\gamma_{\alpha\beta\gamma\delta}E_\gamma E_\delta + \ldots)\mathcal{E}_\beta \ , \tag{2.21}$$

$$H_\alpha = \mu_o^{-1}\beta_\alpha \ . \tag{2.22}$$

Following the eigenvalue approach described in Section 2.1 and using the above expressions for $\underset{\sim}{D}$ and $\underset{\sim}{H}$, one obtains

$$\left[n^2\sigma_\alpha\sigma_\beta - (n^2-1)\delta_{\alpha\beta} + \frac{1}{\varepsilon_o}\alpha_{\alpha\beta} + \frac{1}{2\varepsilon_o}\beta_{\alpha\beta\gamma}E_\gamma + \frac{1}{6\varepsilon_o}\gamma_{\alpha\beta\gamma\delta}E_\gamma E_\delta + \ldots\right]\mathcal{E}_\beta^{(o)} = 0 \ . \tag{2.23}$$

This is the fundamental equation that was derived in eq. (2.14) for describing light propagation, now modified in the presence of an applied low-frequency electric field $\underset{\sim}{E}$.

The three homogeneous equations obtained from eq. (2.23) by letting α = x,y,z in turn yields the matrix equation

$$\begin{bmatrix} n^2(\sigma_x^2 - 1) + 1 + T_{xx} & n^2\sigma_x\sigma_y + T_{xy} & n^2\sigma_x\sigma_z + T_{xz} \\ n^2\sigma_y\sigma_x + T_{yx} & n^2(\sigma_y^2 - 1) + 1 + T_{yy} & n^2\sigma_y\sigma_z + T_{yz} \\ n^2\sigma_z\sigma_x + T_{zx} & n^2\sigma_z\sigma_y + T_{zy} & n^2(\sigma_z^2 - 1) + 1 + T_{zz} \end{bmatrix} \begin{bmatrix} \mathcal{E}_x^{(o)} \\ \mathcal{E}_y^{(o)} \\ \mathcal{E}_z^{(o)} \end{bmatrix} = 0 \ , \tag{2.24}$$

where

$$T_{ij} = \frac{1}{\varepsilon_o}\alpha_{ij} + \frac{1}{2\varepsilon_o}\beta_{ij\gamma}E_\gamma + \frac{1}{6\varepsilon_o}\gamma_{ij\gamma\delta}E_\gamma E_\delta \ . \tag{2.25}$$

The secular equation for determining n is then

$$\begin{vmatrix} n^2(\sigma_x^2 - 1) + 1 + T_{xx} & n^2\sigma_x\sigma_y + T_{xy} & n^2\sigma_x\sigma_z + T_{xz} \\ n^2\sigma_y\sigma_x + T_{yx} & n^2(\sigma_y^2 - 1) + 1 + T_{yy} & n^2\sigma_y\sigma_z + T_{yz} \\ n^2\sigma_z\sigma_x + T_{zx} & n^2\sigma_z\sigma_y + T_{zy} & n^2(\sigma_z^2 - 1) + 1 + T_{zz} \end{vmatrix} = 0 \ . \tag{2.26}$$

It is this equation that will now be used to determine the induced birefringence in KDP which is proportional to the square of an applied electric field.

2.2.2 Special case of the symmetry point group $\bar{4}2m$

Consider the specific case of a KDP crystal which at room temperature belongs to the uniaxial symmetry point group $\bar{4}2m$. This crystal has three mutually perpendicular twofold axes of symmetry, one of which is an improper fourfold axis of symmetry. By convention it is this latter axis that is taken as the 3-axis (optic axis), whilst the two mutually orthogonal twofold axes, in the plane normal to 3, are designated the 1- and 2- axes such that the 1,2,3 axes form a right handed system.

Crystal tensors are traditionally expressed relative to crystallographic Cartesian axes. If the laboratory x,y,z axes are chosen to coincide respectively with the crystal's 1,2,3 axes, then the off-diagonal

components of the polarizability $\alpha_{\alpha\beta}$ are zero since crystallographic axes serve as principal axes for this second rank polar tensor (Birss 1966). For propagation of the light beam along the optic axis, ie $\underset{\sim}{\sigma} = (0,0,1)$, eq. (2.26) may be written as

$$\begin{vmatrix} -n^2 + 1 + T_{xx} & T_{xy} & T_{xz} \\ T_{yx} & -n^2 + 1 + T_{yy} & T_{yz} \\ T_{zx} & T_{zy} & 1 + T_{zz} \end{vmatrix} = 0 \,. \qquad (2.27)$$

Quantum-mechanical results for the polarizability tensor $\alpha_{\alpha\beta}$, given in Section 2.3, show that it is symmetric on interchanging the subscripts α and β. It follows from eq. (2.20) that the hyperpolarizability tensors $\beta_{\alpha\beta\gamma}$ and $\gamma_{\alpha\beta\gamma\delta}$ are likewise symmetric when the subscripts α and β are interchanged, and that $\gamma_{\alpha\beta\gamma\delta}$ is also symmetric in γ and δ. Making use of this intrinsic symmetry as well as of tensor symmetry properties for the symmetry point group $\bar{4}2m$, given in tables by Birss (1966), one may identify the non-vanishing independent components of $\alpha_{\alpha\beta}$, $\beta_{\alpha\beta\gamma}$, and $\gamma_{\alpha\beta\gamma\delta}$, as well as relationships between them, as follows:

$$\alpha_{xx} = \alpha_{yy}, \ \alpha_{zz},$$

$$\beta_{xyz} = \beta_{yxz}, \ \beta_{xzy} = \beta_{zxy} = \beta_{zyx} = \beta_{yzx},$$

$$\gamma_{xxxx} = \gamma_{yyyy}, \ \gamma_{zzzz}, \ \gamma_{xxyy} = \gamma_{yyxx}, \ \gamma_{xyxy} = \gamma_{yxyx} = \gamma_{yxxy} = \gamma_{xyyx},$$

$$\gamma_{yzzy} = \gamma_{zyyz} = \gamma_{zyzy} = \gamma_{yzyz} = \gamma_{xzxz} = \gamma_{zxzx} = \gamma_{xzzx} = \gamma_{zxxz},$$

$$\gamma_{xxzz} = \gamma_{yyzz}, \ \gamma_{zzxx} = \gamma_{zzyy} \qquad (2.28)$$

If $\underset{\sim}{E}$ is taken to be along the x-axis of the crystal, and use is made of the tensor symmetry properties in eqs. (2.28), then the secular equation in eq. (2.27) becomes

$$\begin{vmatrix} -n^2 + 1 + \frac{1}{\varepsilon_o}\alpha_{xx} + \frac{1}{6\varepsilon_o}\gamma_{xxxx}E^2 & 0 & 0 \\ 0 & -n^2 + 1 + \frac{1}{\varepsilon_o}\alpha_{xx} + \frac{1}{6\varepsilon_o}\gamma_{yyxx}E^2 & \frac{1}{2\varepsilon_o}\beta_{yzx}E \\ 0 & \frac{1}{2\varepsilon_o}\beta_{yzx}E & 1 + \frac{1}{\varepsilon_o}\alpha_{zz} + \frac{1}{6\varepsilon_o}\gamma_{zzxx}E^2 \end{vmatrix} = 0 \ . \tag{2.29}$$

From the first row of eq. (2.29) it is evident that

$$\begin{aligned} n_x^2 &= 1 + \frac{1}{\varepsilon_o}\alpha_{xx} + \frac{1}{6\varepsilon_o}\gamma_{xxxx}E^2 \\ &\simeq n_o^2 + \frac{1}{6\varepsilon_o}\gamma_{xxxx}E^2 \ , \end{aligned} \tag{2.30}$$

where n_o is the so-called ordinary index of refraction. It is defined by

$$n_o^2 = 1 + \frac{1}{\varepsilon_o}\alpha_{xx} \ . \tag{2.31}$$

Substituting eq. (2.30) into the equation on which the first row of the determinant in eq. (2.29) is based yields the corresponding eigenvector

$$\underset{\sim}{\mathcal{E}}^{(o)} = (\mathcal{E}^{(o)}, 0, 0) \ .$$

This is linearly polarized parallel to the crystallographic x-axis.

From the sub-determinant in rows two and three in eq. (2.29) one obtains another refractive index given by

$$n_y^2 \simeq n_o^2 + \frac{1}{6\varepsilon_o}\gamma_{yyxx}E^2 - \left(\frac{1}{2n_e\varepsilon_o}\beta_{yzx}E\right)^2 \ , \tag{2.32}$$

where the binomial theorem was used and terms of fourth- and higher-order in the applied field were neglected, in keeping with earlier approximations. In the above equation n_e is the extraordinary refractive index defined by

$$n_e^2 = 1 + \frac{1}{\varepsilon_o}\alpha_{zz} \ . \tag{2.33}$$

When eq. (2.32) is substituted into either the second or third row of eq. (2.29) the corresponding eigenvector is found

$$\frac{\mathcal{E}_z^{(o)}}{\mathcal{E}_y^{(o)}} = -\frac{\frac{1}{2\varepsilon_o}\beta_{yzx}E}{n_e^2 + \frac{1}{6\varepsilon_o}\gamma_{zzxx}E^2} \ . \tag{2.34}$$

From this equation it is apparent that this second eigenvector has a small

component $\mathcal{E}_z^{(o)}$ parallel to the direction of the wave propagation. Consequently, the Poynting vector and $\underset{\sim}{\sigma}$ diverge slightly (Graham & Raab 1990). From knowledge of the order of magnitude of the polarizability tensor β_{yzx} of KDP and the strength of the electric fields used in the experiment it is possible to calculate that $\mathcal{E}_z^{(o)}/\mathcal{E}_y^{(o)}$ is about 10^{-5}. Accordingly, to a good approximation the eigenvector under consideration may be taken to be polarized parallel to the crystallographic y-axis.

For the light propagation and applied field constraints considered, eqs. (2.30) and (2.32) give the change in refractive index of the two polarization eigenvectors due to the application of the electric field as

$$\Delta n_x = n_x - n_o = \frac{1}{12 n_o \varepsilon_o} \gamma_{xxxx} E^2 + O\left(E^4\right) , \tag{2.35}$$

$$\Delta n_y = n_y - n_o = \frac{1}{2n_o}\left[\frac{1}{6\varepsilon_o}\gamma_{yyxx} - \left[\frac{1}{2n_o\varepsilon_o}\beta_{yzx}\right]^2\right]E^2 + O\left(E^4\right) . \tag{2.36}$$

Following the above approach for KDP, but now taking the direction of light propagation to be along the y-axis of the crystal, to which a field is applied in the x-direction, it is possible to determine that two polarization eigenvectors will exist for this propagation direction which have the following refractive indices and eigenvectors:

$$n_x^2 = n_o^2 + \frac{1}{6\varepsilon_o}\gamma_{xxxx}E^2 , \quad \underset{\sim}{\mathcal{E}}^{(o)} = (\mathcal{E}^{(o)}, 0, 0) ,$$
$$n_z^2 = n_e^2 + \frac{1}{6\varepsilon_o}\gamma_{zzxx}E^2 - \left[\frac{1}{2n_o\varepsilon_o}\beta_{yzx}E\right]^2 + O\left(E^4\right) , \quad \mathcal{E}^{(o)} = (0, 0, \mathcal{E}^{(o)}) . \tag{2.37}$$

Accordingly, the change in refractive index of the polarization eigenvector $\underset{\sim}{\mathcal{E}}^{(o)} = (0, 0, \mathcal{E}^{(o)})$ for this configuration on the application of an electric field to the medium is given as

$$\Delta n_z = n_z - n_e = \frac{1}{2n_e}\left[\frac{1}{6\varepsilon_o}\gamma_{zzxx} - \left[\frac{1}{2n_o\varepsilon_o}\beta_{yzx}\right]^2\right]E^2 + O\left(E^4\right) . \tag{2.38}$$

Table 2.1 is presented to display the above theoretical discussion.

Tabulated are the field-induced changes in the refractive indices of the polarization eigenvectors for the light propagation constraints under consideration.

In the above theoretical discussion the assumption that the crystal is optically inactive is implicit. Since KDP belongs to the non-enantiomorphous class of crystals it will not, in principle, exhibit optical activity for light propagation along the optic axis. However, it is optically active for propagation off this axis. With this in mind the optical activity for light propagation along the crystallographic y-axis was checked but found to be negligible relative to the linear birefringence. This conclusion is in agreement with previous findings (see, for example, Kobayashi *et al.* 1988).

Past work in the field of the quadratic electro-optic effects in KDP was conducted on the basis of the formally equivalent method of the index ellipsoid. Accordingly, the literature on this effect in KDP tends to be in terms of the linear and quadratic electro-optic coefficients $r_{\alpha\beta\gamma}$ and $g_{\alpha\beta\gamma\delta}$ defined by means of the electric field-induced changes to the impermeability tensor in eq. (1.14).

It follows from the definition of the impermeability tensor that the first- and second-order hyperpolarizability tensors $\beta_{\alpha\beta\gamma}$ and $\gamma_{\alpha\beta\gamma\delta}$, defined by eq. (2.18), may be expressed in terms of the linear and quadratic electro-optic tensors as (see Appendix A)

$$\frac{1}{2\varepsilon_o}\beta_{ijk} = - n_i^2 n_j^2 r_{ijk} , \qquad (2.39)$$

$$\frac{1}{6\varepsilon_o}\gamma_{ijkl} = - n_i^2 n_j^2 g_{ijkl} , \qquad (2.40)$$

where summation over the indices is no longer implied.

Equations (2.35), (2.36), and (2.38) may be written in terms of the corresponding electro-optic coefficients as

$$\Delta n_x = -\frac{1}{2}n_o^3\, g_{xxxx}E^2 , \tag{2.41}$$

$$\Delta n_y = \frac{1}{2}n_o^3\left[-g_{yyxx} - n_e^2\left(r_{yzx}\right)^2\right]E^2 , \tag{2.42}$$

$$\Delta n_z = \frac{1}{2}n_e^3\left[-g_{zzxx} - n_o^2\left(r_{yzx}\right)^2\right]E^2 . \tag{2.43}$$

It is convenient to describe the changes in refractive index of the polarization eigenvectors for a wave propagating through a medium in terms of changes to the index ellipsoid. The central cross-section of this ellipsoid is taken to be the plane perpendicular to the direction of light-wave propagation. The lengths of the principal semi-axes of this ellipse are measures of the principal refractive indices, and coincide with the directions of the electric induction vectors $\underset{\sim}{D}$.

The length of the ellipse radius for a given α, where α is defined as the angle between the direction of the electric vector of the incident light wave and the crystallographic x-direction, is a measure of the refractive index of the light wave polarized in this direction. Considering a field applied along the crystal's x-axis and the light to be propagating along the crystal's optic axis, one can show by means of eqs. (2.41) and (2.42) that the change in refractive index at an angle α for the ellipsoid cross-section is given by

$$\Delta n(\alpha) = -\frac{1}{2}n_o^3\left[n_e^2[r_{yzx}]^2\sin^2\alpha + g_{xxxx}\cos^2\alpha + g_{yyxx}\sin^2\alpha\right]E^2 . \tag{2.44}$$

Measurements of the change in refractive index of the uniaxial KDP crystal for a light wave propagating along the optic axis polarized at an angle relative to the crystallographic axes, and for the applied field as

considered, should satisfy the above relation.

It is not possible to derive an expression analogous to eq. (2.44) for light propagation along the crystallographic y-axis since the natural birefringence of the KDP crystal for this direction of light propagation forbids a beam polarized at angles off the crystallographic axes to remain linearly polarized. Such light will emerge from the crystal elliptically polarized. The derivation of the eq. (2.44) assumes the retention of linear polarization. In truth, under the presence of an applied field in the x-direction the KDP crystal is birefringent for light propagation along the optic axis, but this birefringence is very small, and to a good approximation eq. (2.44) holds.

2.3 QUANTUM-MECHANICAL EXPRESSIONS FOR POLARIZABILITY TENSORS

The quantum-mechanical expressions for the polarizability tensors given in eqs. (2.7) allow one to deduce certain essential information about them, in particular: relationships between them where they exist, intrinsic symmetry of subscripts, relative orders of magnitude, and effect of an origin shift. These quantum-mechanical expressions may be derived by means of first-order perturbation theory, in which the electromagnetic perturbation Hamiltonian is expressed in the Barron-Gray gauge (Barron & Gray 1973; Raab 1975).

Induced electric and magnetic multipole moments in the n^{th} eigenstate may be obtained from expectation values of the corresponding operators using the perturbed eigenfunction. The quantum-mechanical expectation value of the electric dipole moment density P_α at a macroscopic volume element ΔV which is in quantum state n may be written to first-order in the light-wave perturbation as

$$\begin{aligned}\langle P_\alpha\rangle_n &= \langle n(t)|P_\alpha|n(t)\rangle \\ &= \langle n^{(o)}(t) + n^{(1)}(t) + \ldots|P_\alpha|n^{(o)}(t) + n^{(1)}(t) + \ldots\rangle \\ &= \langle P_\alpha^{(o)}\rangle + 2\mathcal{R}e\langle n^{(o)}(t)|P_\alpha|n^{(1)}(t)\rangle + \ldots \ . \end{aligned} \tag{2.45}$$

Since any state of a system may be expressed as a linear combination of the eigenstates of a hermitian operator, we write

$$|n^{(1)}(t)\rangle = \sum_j a_j(t)|j^{(o)}(t)\rangle \ . \tag{2.46}$$

Then from time-dependent perturbation theory it may be shown for $j \neq n$ that

$$a_j(t) = -\frac{i}{\hbar}\int_o^t e^{-i\omega_{nj}t}H_{jn}^{(1)}\,dt \ , \tag{2.47}$$

where

$$\omega_{nj} = \left[E_n^{(o)} - E_j^{(o)}\right]/\hbar \ . \tag{2.48}$$

In the above $H_{jn}^{(1)}$ denotes the matrix element of the first-order perturbation Hamiltonian between the time-independent unperturbed states, namely

$$\left\langle j^{(o)}(0)\left|H^{(1)}\right|n^{(o)}(0)\right\rangle .$$

Equation (2.45) may thus be written as

$$\begin{aligned}\langle P_\alpha\rangle_n &= \left\langle n^{(o)}(0)e^{-iE_n^{(o)}t/\hbar}|P_\alpha|n^{(o)}(0)e^{-iE_n^{(o)}t/\hbar}\right\rangle \\ &\quad + 2\mathcal{R}e\sum_{j\neq n}a_j(t)\left\langle n^{(o)}(0)e^{-iE_n^{(o)}t/\hbar}|P_\alpha|j^{(o)}(0)e^{-iE_j^{(o)}t/\hbar}\right\rangle + \ldots \\ &= \left\langle P_\alpha^{(o)}\right\rangle + 2\mathcal{R}e\sum_{j\neq n}a_j(t)e^{i\omega_{nj}t}\left\langle n^{(o)}(0)|P_\alpha|j^{(o)}(0)\right\rangle + \ldots \ . \end{aligned} \tag{2.49}$$

The semi-classical Hamiltonian for describing a system such as the macroscopic volume element ΔV in an electromagnetic field is

$$H = \sum\frac{1}{2m}\left(\underset{\sim}{p} - q\underset{\sim}{A}\right)^2 + V + \sum q\phi \ , \tag{2.50}$$

where q is the charge of a particle in ΔV with mass m and momentum operator $\underset{\sim}{p}$, and V is the unperturbed potential energy operator. $\underset{\sim}{A}$ and ϕ are potentials at charge q which, for a source-free region of space, Barron and

Gray (1973) postulated as

$$A_\alpha(\underset{\sim}{r},t) = \varepsilon_{\alpha\beta\gamma}\left\{\frac{1}{2}\left[\mathcal{B}_\beta(\underset{\sim}{r},t)\right]_o r_\gamma + \frac{1}{3}\left[\nabla_\delta \mathcal{B}_\beta(\underset{\sim}{r},t)\right]_o r_\gamma r_\delta + \frac{1}{6}\left[\nabla_\varepsilon \nabla_\delta \mathcal{B}_\beta(\underset{\sim}{r},t)\right]_o r_\gamma r_\delta r_\varepsilon + \ldots\right\} \quad (2.51)$$

and

$$\phi(\underset{\sim}{r},t) = \left[\phi(\underset{\sim}{r},t)\right]_o - \left[\mathcal{E}_\alpha(\underset{\sim}{r},t)\right]_o r_\alpha - \frac{1}{2}\left[\nabla_\beta \mathcal{E}_\alpha(\underset{\sim}{r},t)\right]_o r_\alpha r_\beta - \ldots , \quad (2.52)$$

where $[\ ]_o$ denotes the origin value of an expression. By means of these expressions the Hamiltonian in eq. (2.50) may be rewritten as

$$H = \sum \frac{1}{2m}\underset{\sim}{p}^2 + V + q\phi - p_\alpha(\mathcal{E}_\alpha)_o - \frac{1}{2}q_{\alpha\beta}(\nabla_\beta \mathcal{E}_\alpha)_o - \frac{1}{6}q_{\alpha\beta\gamma}(\nabla_\gamma \nabla_\beta \mathcal{E}_\alpha)_o - \ldots - m_\alpha(\mathcal{B}_\alpha)_o - \frac{1}{2}m_{\alpha\beta}(\nabla_\beta \mathcal{B}_\alpha)_o - \ldots . \quad (2.53)$$

In this Hamiltonian p_α, $q_{\alpha\beta}$, $q_{\alpha\beta\gamma}$, m_α, and $m_{\alpha\beta}$ are the quantum-mechanical multipole moment operators of the macroscopic volume element, corresponding to the classical multipole moments defined in eqs. (2.6).

The first-order perturbation Hamiltonian in the electric octopole-magnetic quadrupole approximation is thus given by (Raab 1975)

$$H^{(1)} = q\phi - p_\alpha(\mathcal{E}_\alpha)_o - \frac{1}{2}q_{\alpha\beta}(\nabla_\beta \mathcal{E}_\alpha)_o - \frac{1}{6}q_{\alpha\beta\gamma}(\nabla_\gamma \nabla_\beta \mathcal{E}_\alpha)_o - m_\alpha(\mathcal{B}_\alpha)_o - \frac{1}{2}m_{\alpha\beta}(\nabla_\beta \mathcal{B}_\alpha)_o - \ldots . \quad (2.54)$$

The Barron and Gray gauge choices thus allow the first-order perturbation Hamiltonian to be cast in an explicit multipole form, unlike the more common gauges due to Lorentz and Coulomb. Then from eqs. (2.47) and (2.54)

$$a_j(t) = -\frac{i}{\hbar}\int_o^t e^{-i\omega_{nj}t}\left[q_{j_n}\phi - p_{\alpha_{j_n}}(\mathcal{E}_\alpha)_o - \frac{1}{2}q_{\alpha\beta_{j_n}}(\nabla_\beta \mathcal{E}_\alpha)_o - \frac{1}{6}q_{\alpha\beta\gamma_{j_n}}(\nabla_\gamma \nabla_\beta \mathcal{E}_\alpha)_o - m_{\alpha_{j_n}}(\mathcal{B}_\alpha)_o - \frac{1}{2}m_{\alpha\beta_{j_n}}(\nabla_\beta \mathcal{B}_\alpha)_o - \ldots\right] dt . \quad (2.55)$$

$\underset{\sim}{\mathcal{E}}$ may be written explicitly in the form

$$\underset{\sim}{\mathcal{E}} = \underset{\sim}{\mathcal{E}}^{(o)} \cos\omega[t - n\underset{\sim}{r}.\underset{\sim}{\sigma}/c] , \quad (2.56)$$

and $\underset{\sim}{\mathcal{B}}$ in terms of $\underset{\sim}{\mathcal{E}}$ has, from eq. (2.13), been shown to be

$$\mathcal{B}_\alpha = \frac{n}{c}\varepsilon_{\alpha\beta\gamma}\sigma_\beta \mathcal{E}_\gamma .$$

Substituting these expressions into eq. (2.55) and using the following integrals:

$$\int_0^t e^{-i\omega_{nj}t}\cos\omega t\ dt = -\frac{ie^{-i\omega_{nj}t}}{\omega^2 - \omega_{nj}^2}[\omega_{nj}\cos\omega t + i\omega\sin\omega t] \tag{2.57}$$

and

$$\int_0^t e^{-i\omega_{nj}t}\sin\omega t\ dt = \frac{ie^{-i\omega_{nj}t}}{\omega^2 - \omega_{nj}^2}[i\omega\cos\omega t - \omega_{nj}\sin\omega t]\ , \tag{2.58}$$

yield

$$\begin{aligned} a_j(t) = \frac{1}{\hbar}\frac{e^{-i\omega_{nj}t}}{\omega^2 - \omega_{nj}^2}\Big[& p_{\alpha}{}_{jn}\left[\omega_{nj}(\mathcal{E}_\alpha)_0 - i(\dot{\mathcal{E}}_\alpha)_0\right] + \frac{1}{2}q_{\alpha\beta}{}_{jn}\left[\omega_{nj}(\nabla_\beta\mathcal{E}_\alpha)_0 - i(\nabla_\beta\dot{\mathcal{E}}_\alpha)_0\right] \\ & + \frac{1}{6}q_{\alpha\beta\gamma}{}_{jn}\left[\omega_{nj}(\nabla_\gamma\nabla_\beta\mathcal{E}_\alpha)_0 - i(\nabla_\gamma\nabla_\beta\dot{\mathcal{E}}_\alpha)_0\right] + m_{\alpha}{}_{jn}\left[\omega_{nj}(\mathcal{B}_\alpha)_0 - i(\dot{\mathcal{B}}_\alpha)_0\right] \\ & + \frac{1}{2}m_{\alpha\beta}{}_{jn}\left[\omega_{nj}(\nabla_\beta\mathcal{B}_\alpha)_0 - i(\nabla_\beta\dot{\mathcal{B}}_\alpha)_0\right] + \ldots\Big]\ . \end{aligned} \tag{2.59}$$

It follows from eqs. (2.49) and (2.59) that

$$\begin{aligned} \langle P_\alpha\rangle_n = P_{\alpha}{}_{nn} + \frac{2}{\hbar}\sum_{j\neq n}\frac{1}{\omega^2 - \omega_{nj}^2}\mathcal{R}e\Big\{P_{\alpha}{}_{nj}\Big[& p_{\beta}{}_{jn}\left[\omega_{nj}(\mathcal{E}_\beta)_0 - i(\dot{\mathcal{E}}_\beta)_0\right] \\ & + \frac{1}{2}q_{\beta\gamma}{}_{jn}\left[\omega_{nj}(\nabla_\gamma\mathcal{E}_\beta)_0 - i(\nabla_\gamma\dot{\mathcal{E}}_\beta)_0\right] + \frac{1}{6}q_{\beta\gamma\delta}{}_{jn}\left[\omega_{nj}(\nabla_\delta\nabla_\gamma\mathcal{E}_\beta)_0 - i(\nabla_\delta\nabla_\gamma\dot{\mathcal{E}}_\beta)_0\right] \\ & + m_{\beta}{}_{jn}\left[\omega_{nj}(\mathcal{B}_\beta)_0 - i(\dot{\mathcal{B}}_\beta)_0\right] + \frac{1}{2}m_{\beta\gamma}{}_{jn}\left[\omega_{nj}(\nabla_\gamma\mathcal{B}_\beta)_0 - i(\nabla_\gamma\dot{\mathcal{B}}_\beta)_0\right] + \ldots\Big]\Big\}\ . \end{aligned} \tag{2.60}$$

The classical expression for the electric dipole moment per unit macroscopic volume induced by the fields $\underset{\sim}{\mathcal{E}}$ and $\underset{\sim}{\mathcal{B}}$ of a light wave, and also by their space and time derivatives, is, to the order of electric octopoles and magnetic quadrupoles,

$$\begin{aligned} P_\alpha = P_\alpha^{(o)} + \alpha_{\alpha\beta}(\mathcal{E}_\beta)_0 + \frac{1}{\omega}\alpha'_{\alpha\beta}(\dot{\mathcal{E}}_\beta)_0 + \frac{1}{2}a_{\alpha\beta\gamma}(\nabla_\gamma\mathcal{E}_\beta)_0 + \frac{1}{2\omega}a'_{\alpha\beta\gamma}(\nabla_\gamma\dot{\mathcal{E}}_\beta)_0 \\ + \frac{1}{6}b_{\alpha\beta\gamma\delta}(\nabla_\delta\nabla_\gamma\mathcal{E}_\beta)_0 + \frac{1}{6\omega}b'_{\alpha\beta\gamma\delta}(\nabla_\delta\nabla_\gamma\dot{\mathcal{E}}_\beta)_0 + \ldots + G_{\alpha\beta}(\mathcal{B}_\beta)_0 + \frac{1}{\omega}G'_{\alpha\beta}(\dot{\mathcal{B}}_\beta)_0 \\ + \frac{1}{2}H_{\alpha\beta\gamma}(\nabla_\gamma\mathcal{B}_\beta)_0 + \frac{1}{2\omega}H'_{\alpha\beta\gamma}(\nabla_\gamma\dot{\mathcal{B}}_\beta)_0 + \ldots\ . \end{aligned} \tag{2.61}$$

Comparison of the classical and quantum-mechanical expansions given above yield a quantum-mechanical expression for the polarizability tensor $\alpha_{\alpha\beta}$ of

the macroscopic volume element, namely

$$\alpha_{\alpha\beta} = \frac{2}{\hbar}\sum_{j\neq n} Z_{jn}\omega_{jn}\mathcal{R}e\left(\langle n|p_\alpha|j\rangle\langle j|P_\beta|n\rangle\right) = \alpha_{\beta\alpha} .$$

In terms of the definition $\underset{\sim}{P} = \underset{\sim}{p}/\Delta V$, this may be written as

$$\alpha_{\alpha\beta} = \frac{2}{\hbar}\Delta V\sum_{j\neq n} Z_{jn}\omega_{jn}\mathcal{R}e\left(\langle n|P_\alpha|j\rangle\langle j|P_\beta|n\rangle\right) = \alpha_{\beta\alpha} .$$

The permutation symmetry of the subscripts is a consequence of the hermitian nature of $\underset{\sim}{P}$. In the above $\omega_{jn} = -\omega_{nj}$ was used. Also $Z_{jn} = (\omega_{jn}^2 - \omega^2)^{-1}$ is a line-shape function which, where relevant, may be modified to allow for absorption (Buckingham & Stephens 1966; Weisskopf & Wigner 1930).

Quantum-mechanical expressions for the other polarizability tensors are

$$\alpha'_{\alpha\beta} = -\frac{2}{\hbar}\Delta V\sum_{j\neq n} Z_{jn}\omega\mathcal{I}m\left(\langle n|P_\alpha|j\rangle\langle j|P_\beta|n\rangle\right) = -\alpha'_{\beta\alpha} ,$$

$$a_{\alpha\beta\gamma} = \frac{2}{\hbar}\Delta V\sum_{j\neq n} Z_{jn}\omega_{jn}\mathcal{R}e\left(\langle n|P_\alpha|j\rangle\langle j|Q_{\beta\gamma}|n\rangle\right) = a_{\alpha\gamma\beta} ,$$

$$a'_{\alpha\beta\gamma} = -\frac{2}{\hbar}\Delta V\sum_{j\neq n} Z_{jn}\omega\mathcal{I}m\left(\langle n|P_\alpha|j\rangle\langle j|Q_{\beta\gamma}|n\rangle\right) = a'_{\alpha\gamma\beta} ,$$

$$b_{\alpha\beta\gamma\delta} = \frac{2}{\hbar}\Delta V\sum_{j\neq n} Z_{jn}\omega_{jn}\mathcal{R}e\left(\langle n|P_\alpha|j\rangle\langle j|Q_{\beta\gamma\delta}|n\rangle\right) = b_{\alpha\gamma\beta\delta} = b_{\alpha\beta\delta\gamma} = b_{\alpha\delta\gamma\beta} ,$$

$$b'_{\alpha\beta\gamma\delta} = -\frac{2}{\hbar}\Delta V\sum_{j\neq n} Z_{jn}\omega\mathcal{I}m\left(\langle n|P_\alpha|j\rangle\langle j|Q_{\beta\gamma\delta}|n\rangle\right) = b'_{\alpha\gamma\beta\delta} = b'_{\alpha\beta\delta\gamma} = b'_{\alpha\delta\gamma\beta} ,$$

$$G_{\alpha\beta} = \frac{2}{\hbar}\Delta V\sum_{j\neq n} Z_{jn}\omega_{jn}\mathcal{R}e\left(\langle n|P_\alpha|j\rangle\langle j|M_\beta|n\rangle\right) ,$$

$$G'_{\alpha\beta} = -\frac{2}{\hbar}\Delta V\sum_{j\neq n} Z_{jn}\omega\mathcal{I}m\left(\langle n|P_\alpha|j\rangle\langle j|M_\beta|n\rangle\right) ,$$

$$H_{\alpha\beta\gamma} = \frac{2}{\hbar}\Delta V\sum_{j\neq n} Z_{jn}\omega_{jn}\mathcal{R}e\left(\langle n|P_\alpha|j\rangle\langle j|M_{\beta\gamma}|n\rangle\right) ,$$

$$H'_{\alpha\beta\gamma} = -\frac{2}{\hbar}\Delta V\sum_{j\neq n} Z_{jn}\omega\mathcal{I}m\left(\langle n|P_\alpha|j\rangle\langle j|M_{\beta\gamma}|n\rangle\right) .$$

In a similar way the quantum-mechanical expressions for the polarizability tensors in the expansions of $Q_{\alpha\beta}$, $Q_{\alpha\beta\gamma}$, M_α, and $M_{\alpha\beta}$ in eqs. (2.7) can be found. They are

$$a_{\alpha\beta\gamma} = \frac{2}{\hbar}\Delta V \sum_{j\neq n} Z_{jn}\omega_{jn}\mathcal{R}e\left(\langle n|Q_{\alpha\beta}|j\rangle\langle j|P_\gamma|n\rangle\right) = a_{\gamma\alpha\beta} ,$$

$$a'_{\alpha\beta\gamma} = -\frac{2}{\hbar}\Delta V \sum_{j\neq n} Z_{jn}\omega\mathcal{I}m\left(\langle n|Q_{\alpha\beta}|j\rangle\langle j|P_\gamma|n\rangle\right) = -a'_{\gamma\alpha\beta} ,$$

$$d_{\alpha\beta\gamma\delta} = \frac{2}{\hbar}\Delta V \sum_{j\neq n} Z_{jn}\omega_{jn}\mathcal{R}e\left(\langle n|Q_{\alpha\beta}|j\rangle\langle j|Q_{\gamma\delta}|n\rangle\right) = d_{\beta\alpha\delta\gamma} = d_{\gamma\delta\alpha\beta} ,$$

$$d'_{\alpha\beta\gamma\delta} = -\frac{2}{\hbar}\Delta V \sum_{j\neq n} Z_{jn}\omega\mathcal{I}m\left(\langle n|Q_{\alpha\beta}|j\rangle\langle j|Q_{\gamma\delta}|n\rangle\right) = -d'_{\beta\alpha\delta\gamma} = -d'_{\gamma\delta\alpha\beta} ,$$

$$L_{\alpha\beta\gamma} = \frac{2}{\hbar}\Delta V \sum_{j\neq n} Z_{jn}\omega_{jn}\mathcal{R}e\left(\langle n|Q_{\alpha\beta}|j\rangle\langle j|M_\gamma|n\rangle\right) ,$$

$$L'_{\alpha\beta\gamma} = -\frac{2}{\hbar}\Delta V \sum_{j\neq n} Z_{jn}\omega\mathcal{I}m\left(\langle n|Q_{\alpha\beta}|j\rangle\langle j|M_\gamma|n\rangle\right) ,$$

$$b_{\alpha\beta\gamma\delta} = \frac{2}{\hbar}\Delta V \sum_{j\neq n} Z_{jn}\omega_{jn}\mathcal{R}e\left(\langle n|Q_{\alpha\beta\gamma}|j\rangle\langle j|P_\delta|n\rangle\right) = b_{\delta\alpha\beta\gamma} ,$$

$$b'_{\alpha\beta\gamma\delta} = -\frac{2}{\hbar}\Delta V \sum_{j\neq n} Z_{jn}\omega\mathcal{I}m\left(\langle n|Q_{\alpha\beta\gamma}|j\rangle\langle j|P_\delta|n\rangle\right) = -b'_{\delta\alpha\beta\gamma} ,$$

$$G_{\alpha\beta} = \frac{2}{\hbar}\Delta V \sum_{j\neq n} Z_{jn}\omega_{jn}\mathcal{R}e\left(\langle n|M_\alpha|j\rangle\langle j|P_\beta|n\rangle\right) = G_{\beta\alpha} ,$$

$$G'_{\alpha\beta} = -\frac{2}{\hbar}\Delta V \sum_{j\neq n} Z_{jn}\omega\mathcal{I}m\left(\langle n|M_\alpha|j\rangle\langle j|P_\beta|n\rangle\right) = -G'_{\beta\alpha} ,$$

$$\mathcal{L}_{\alpha\beta\gamma} = \frac{2}{\hbar}\Delta V \sum_{j\neq n} Z_{jn}\omega_{jn}\mathcal{R}e\left(\langle n|M_\alpha|j\rangle\langle j|Q_{\beta\gamma}|n\rangle\right) = L_{\beta\gamma\alpha} ,$$

$$\mathcal{L}'_{\alpha\beta\gamma} = -\frac{2}{\hbar}\Delta V \sum_{j\neq n} Z_{jn}\omega\mathcal{I}m\left(\langle n|M_\alpha|j\rangle\langle j|Q_{\beta\gamma}|n\rangle\right) = -L'_{\beta\gamma\alpha} ,$$

$$\mathcal{H}_{\alpha\beta\gamma} = \frac{2}{\hbar}\Delta V \sum_{j\neq n} Z_{jn}\omega_{jn}\mathcal{R}e\left(\langle n|M_{\alpha\beta}|j\rangle\langle j|P_\gamma|n\rangle\right) = H_{\gamma\alpha\beta} ,$$

$$\mathcal{H}'_{\alpha\beta\gamma} = -\frac{2}{\hbar}\Delta V \sum_{j\neq n} Z_{jn}\omega\mathcal{I}m\left(\langle n|M_{\alpha\beta}|j\rangle\langle j|P_\gamma|n\rangle\right) = -H'_{\gamma\alpha\beta} ,$$

$$\chi_{\alpha\beta} = \frac{2}{\hbar}\Delta V \sum_{j\neq n} Z_{jn}\omega_{jn}\mathcal{R}e\left(\langle n|M_\alpha|j\rangle\langle j|M_\beta|n\rangle\right) = \chi_{\beta\alpha} ,$$

$$\chi'_{\alpha\beta} = -\frac{2}{\hbar}\Delta V \sum_{j\neq n} Z_{jn}\omega\mathcal{I}m\left(\langle n|M_\alpha|j\rangle\langle j|M_\beta|n\rangle\right) = -\chi'_{\beta\alpha} .$$

From these expressions it is possible to deduce relationships between polarizability tensors as well as any symmetry in their tensor subscripts, and these are shown above.

CHAPTER THREE

DESCRIPTION OF APPARATUS

3.1 INTRODUCTION

The Michelson interferometer is a well-known scientific instrument which has been used extensively to obtain accurate and reliable experimental results in a wide range of applications. In this experiment such an interferometer, with a sensitivity of 1×10^{-10} m, was used to determine the quadratic electro-optic coefficients $g_{xxxx} = g_{yyyy}$, $g_{xxyy} = g_{yyxx}$, and $g_{zzxx} = g_{zzyy}$, for a KDP crystal.

The intensity of the interference pattern formed by an interferometer is dependent on the optical path length difference of the two beams traversing the two arms of the interferometer. It is possible, by means of a photodiode, to detect the variation in intensity of the interference pattern and thus determine the change in path length, or shift in phase, of the optical beam responsible for the intensity change.

The change in refractive index of a medium through which a light wave propagates will result in a shift in the phase of that beam. Since the electro-optic effect leads to a change in refractive index it was proposed to use a Michelson interferometer to measure the shift in phase of an interferometer beam which passes through an electro-optic medium to which a field is applied. In order to obtain a measure of the sign and magnitude of this induced phase shift, the field-induced path-length difference was compensated for by a known phase shift resulting from the application of an electric field to a ceramic reference sample for which the piezoelectric response had been determined, and to which the mirror in the other arm of

the interferometer was attached. Hence the field-induced change in refractive index of the medium, and subsequently its electro-optic effect, could be determined.

In this research the interferometer beam was propagated, in turn, along the crystallographic y- and z-axes of a KDP crystal to which an electric field was applied in the x-direction. This led to a change in the optical path length, in that arm of the interferometer, which was dependent on the quadratic electro-optic effect. The particular components of the quadratic electro-optic tensor responsible for the observed effect, for the light propagation and applied field directions considered, were shown in Section 2.2 to be g_{xxxx}, g_{yyxx}, and g_{zzxx}. Consequently these coefficients could be determined by the proposed technique.

3.2 THE EXPERIMENTAL ARRANGEMENT

The experimental arrangement for the phase-compensation method proposed is shown schematically in Figure 3.1. In the discussion that follows a detailed analysis of both the experimental arrangement and individual components is presented.

3.2.1 The source of polarized light

A He-Ne laser (Spectra-Physics model 105-1), with a 10 mW intensity and wavelength of 632.8 nm, was used as a source of linearly polarized light for the Michelson interferometer. It was found that over the distance of the interferometer, this beam did not diverge appreciably.

The fast and slow axes of the quarter-wave plate were oriented at 45° to the plane of polarization of the laser beam. Consequently, the light wave

passing through the quarter-wave plate was converted to circular polarization. This quarter-wave plate was cut from a 25 mm diameter mica disc, selected for 632.8 nm, and was mounted in a divided circle, with a resolution of 2′ of arc, to allow for accurate orientation of the plate. Light transmitted through the quarter-wave plate was then passed through a Glan-Taylor polarizing prism, also mounted in a divided circle, which could be rotated through 360°. By rotating the polarizing prism the light propagating in the interferometer could be set to any desired linear polarization.

3.2.2 The beam splitter

The beam splitter consisted of a transparent plane-parallel plate, slightly silvered on the one side, which directed light of equal intensity down the two arms of the interferometer. In order for the path length in glass of the rays to be equal, it was necessary to place in the one beam an unsilvered plate identical to that used in the beam splitter.

The beam splitter was found to display a small amount of anisotropy in that both vertically and horizontally polarized light were transmitted without any depolarization, whilst light polarized at an intermediate angle tended to be depolarized to a small extent. When only this depolarized component was allowed to pass through the crystal, its intensity was far too weak to lead to any measurable electro-optic effect, even for voltages applied to the crystal far greater than those used in the experiment. It was determined experimentally that no depolarization of the interferometer beam occurred on transmission through the crystal sample, its oil bath, and on reflection from the mirrors in either arm of the interferometer.

3.2.3 The crystal and reference samples, and the detection system

In the one arm of the interferometer the beam was reflected back along its path by a plane mirror fixed to the surface of a reference sample with a known piezoelectric response. Light in the other arm passed through a KDP crystal which was submerged in a silicon oil bath (placing KDP in oil was necessary since it is hygroscopic), and was then reflected back along its path by a fixed, highly polished, plane mirror. The reference sample and crystal are discussed separately, and in more detail, later in this chapter.

The two beams emerging from the Michelson interferometer were made to form an interference fringe at the circular aperture in front of the photodiode. These fringes were manipulated by adjusting the interferometer mirrors, in order to achieve the widest spacing between them. This spacing was typically 4 mm. More attention will be given to the detection system later.

3.3 STABILIZATION OF THE MICHELSON INTERFEROMETER

The proposed compensation method for this investigation involves measuring very small phase shifts. With such an experimental technique it is important to ensure that the interferometer, and its components, are isolated from mechanical vibrations due to outside influences. With this in mind, a number of precautions were taken in the construction of the interferometer and its components.

In order to provide sufficient isolation from mechanical vibrations, the optical bench was positioned on an anti-vibration mat which was in turn placed on a slate slab (1.20×0.90×0.05 m^3) supported by five air cushions. In addition, thin flexible copper wires 40 mm long and 0.14 mm in diameter

were used to form electrical contacts to the reference sample and crystal electrodes. The intention of these wires was twofold: firstly, to provide for isolation of the samples from their respective coaxial cables to the voltage supplies, and secondly to ensure the least possible amount of mechanical force was applied to the samples. Isolating the samples from the coaxial cable is important since alternating Coulomb forces along the length of the cables can cause them to vibrate. Tests were made using a microscope to determine whether the copper wires vibrated, but even at the highest voltages used in the research no such effect was observed.

All the optical components were clamped to the optical bench by means of stands, the heights of which were adjustable. A screw gauge on each provided for accurate alignment of the components along the bench. The apparatus, assembled in this manner, was operated in an isolated room with no machinery working nearby.

3.4 THE KDP CRYSTALS

3.4.1 General description

In this research measurements were performed on two mechanically-free KDP crystals at room temperature. These were right parallelepiped in shape and had dimensions of approximately 50x50x5.0 mm^3 (length x width x thickness) and 38x30x6.2 mm^3 respectively. They were cut with their plane surfaces perpendicular to the three crystallographic planes, and in both crystals the two larger plane surfaces were parallel to either the xz- or yz-plane. It was these surfaces that were covered with a thin coat of conducting paint of low resistance in order to produce two electrodes to which a voltage could be applied.

A voltage applied across the crystal electrodes resulted in an electric field in the crystal which was, to the accuracy of the crystal cutting, parallel to either the crystallographic x- or y-axis. As these axes are indistinguishable for the symmetry point group $\bar{4}2m$, it was decided that for the purpose of this experiment the field would be considered to be in the x-direction. Stray fields in the vicinity of the crystal were kept to a minimum by the use of coaxial cables and short copper wires to each electrode. As relative changes in the position of the coaxial cable and sample did not affect readings in any way, it was concluded that the effects of stray fields could be neglected.

On account of KDP being hygroscopic it was necessary to place the crystal in a moisture-free environment. In this experiment the sample was placed in a bath containing optically inactive silicon oil. This bath was constructed of Perspex and had a length and width of 100 mm by 60 mm and was 50 mm deep. Windows, made of thin microscope cover slides, were mounted in its sides to allowed free transmission of the light through the bath. The whole unit was attached to a plate which could be accurately aligned through the use of three screw gauges independently displacing the bath in three mutually orthogonal directions. This facilitated the directing of the beam along the desired crystallographic axis.

3.4.2 Orientation of the crystal samples

Orientating the beam along the crystallographic z-axis was achieved by placing the crystal, in its oil bath, between two crossed polarizers and observing the transmitted beam projected onto a plane screen. A conoscopic image is formed when a uniaxial crystal is illuminated by a monochromatic light wave travelling along its optic axis. This picture consists of

alternating dark and illuminated circles (referred to as isochrome rings) and a black cross (formed by two isogyres) centered on the rings. The birefringence and lengths of the crystals used in this experiment were such that they gave conoscopic images with closely packed isochromes and a well defined isogyre cross. When the incident light wave propagates directly along the optic axis of the crystal the middle of the isogyre cross (called the melatope) coincides with the centre of the field of vision. The bath was orientated until this was achieved. It was necessary to check routinely the crystal alignment by this method between readings to ensure that no changes had occurred.

No isogyre cross is present for light propagating perpendicular to the optic axis of the uniaxial KDP crystal. In order to align the crystal for this direction of light propagation, a less accurate method was adopted whereby the crystal was orientated until the laser beam reflected from its two plane surfaces perpendicular to the y-axis coincide with the incident path. To the accuracy of the crystal cutting, the light was then considered to be propagating along the crystallographic y-axis.

3.4.3 Alignment of crystal axes

For the purpose of this experiment it was necessary to know the angle of linear polarization of the beam incident on the crystal relative to the crystallographic axes.

To achieve this a quarter-wave plate and Glan-Taylor polarizing prism were temporarily included in the interferometer arrangement being placed in the beam after the KDP crystal, where the light wave propagated along the crystallographic z-axis. The transmission axis of this second polarizer was

set at 90°, and the fast and slow axes of the quarter-wave plate set at 45°, to the linearly polarized beam incident on the crystal. A photodiode was then used to detect the intensity of the beam transmitted through the crystal and these optical components. This resulted in the arrangement shown in Figure 1.1. Under these circumstances eq. (1.15) for the relative intensity of the transmitted beam in such a system reduces to

$$I/I_0 = - \sin(2\alpha)\sin(2[\alpha-90])\sin^2(\Delta\Gamma) \ , \qquad (3.1)$$

where α is the angle of the incident light linear polarization with respect to the crystallographic axes, and $\Delta\Gamma$ is the total phase shift. As an alternating voltage was applied to the crystal this led to an alternating phase shift and thus modulation in the relative light intensity.

With a constant ac voltage applied along the x-axis of the KDP crystal a lock-in amplifier was used to detect the modulation intensity at the frequency of the applied voltage. On rotating the plane of linear polarization of the light incident on the crystal, and keeping the transmission axis of the second polarizer at 90° and the fast and slow axes of the quarter-wave plate at 45°, this modulation intensity was found to vary in magnitude. For a KDP crystal and the particular constraints being considered, the modulation intensity detected at the fundamental frequency can be shown from eq. (3.1) to have a maximum when the incident beam is linearly polarized at 45° to the crystallographic axes (Górski *et al.* 1994). Accordingly, this maximum could be determined and the angle of the linear polarization of the incident beam could be found with respect to the crystallographic axes. When rotating the crystal in order to allow for light propagation along the crystallographic y-axis, care was taken to rotate the crystal in a plane about the x-axis.

3.4.4 Measurement of the voltage applied to the crystal

The Philips wave synthesizer (model PM 5190) provided an ac signal of 50 mV rms which was fed into the high voltage amplifier allowing voltages of up to 4000 V rms to be applied across the crystal. The output of the high-voltage amplifier was maintained to within about 0.1 % of the preset value by means of a feedback circuit which was incorporated within the amplifier.

The quadratic electro-optic effects described by the three coefficients g_{xxxx}, g_{yyxx}, and g_{zzxx}, which are to be measured in this experiment, are typically very small. Accordingly it is necessary to apply large modulation voltages to the crystal in order to induce measurable effects. A high-voltage probe for measuring these voltages was available only for a limited period and consequently an alternative procedure was devised as follows.

A 1 kΩ resistor was connected in series with the crystal. The ratio of the voltage drop across the resistor, measured on a Hewlett-Packard model 3478A multimeter, to that across the crystal, as determined by the high-voltage probe, was found to be constant over the range of voltages used in this experiment. This preliminary test with the probe gave confidence to the procedure used throughout all subsequent measurements which also relied on a constant ratio. For particular orientations of the crystal a measurable quadratic electro-optic effect was attainable with modulation voltages of the order of 1000 V rms. With a 0 to 1000 V rms Escort multimeter (model EDM 2347) connected across the crystal, giving a precise value for its voltage, the compensation approach described in Section 4.1 was used to determine the electro-optic effect. On disconnecting the Escort voltmeter

but otherwise leaving the crystal orientation unaltered, and with the multimeter across the 1 kΩ resistor, a voltage of similar but now unknown magnitude was applied to the crystal and the compensation procedure repeated. This, together with the known magnitude of the electro-optic effect, allowed the voltage across the crystal to be calculated and then compared with that across the 1 kΩ resistor. This comparison was repeated a number of times for each of the two crystals studied. Higher voltages on the crystal were determined from the measured potential drop across the resistor, assuming firstly the same ratio as was found with the crystal voltage of about 1000 V and secondly that the constancy of this ratio held at the higher voltages used, as confirmed by the preliminary test with the high-voltage probe.

Based on the scatter in the results obtained for the electro-optic coefficients by the compensation approach, which leads to a far greater uncertainty in the calibration than the precision of the voltage readings given by either multimeters used, the uncertainty in the voltage determined in this way was estimated to be within 5%.

3.5 THE REFERENCE SAMPLES

In the experiment two different types of reference sample were used, the first being quartz discs 5 mm thick and with a diameter of 15 mm. The disc faces were cut perpendicular to the crystallographic x-axis and, once polished, were flash-coated with aluminium to provide electrodes on each face which were also reflecting. A voltage applied across these plates resulted in a field along the x-axis of the quartz to the accuracy of the cutting of the crystal.

In the interferometer the quartz plates were oriented perpendicular to the incident light beam, so reflecting the beam back along its path. Hence the only change in the light's path length resulted from a change in the crystal dimension in the crystallographic x-direction. The piezoelectric coefficient responsible for this change when a field is applied to the plates is d_{xxx}, the magnitude of which for quartz has been measured extensively and a recommended value of 2.3×10^{-12} mV^{-1} given by Landolt-Börnstein (1979).

For the other reference sample a ceramic disc was used which exhibited a large piezoelectric effect. This disc was approximately 3 mm thick and had a diameter of 16 mm. A small, highly polished, plane mirror was placed on one of the ceramic's faces, both of which had thin conducting coats covering the surfaces which formed two electrodes. In the experimental arrangement this disc was placed in an arm of the interferometer and the beam was reflected off the mirror attached to its surface. A voltage applied across the electrodes resulted in a field-induced strain, which led to a change in the ceramic's dimensions, due to its piezoelectric effect, in the direction of the interferometer beam. This resulted in a change in the optical path length of the radiation in that arm of the interferometer.

The experimental results obtained when using both quartz samples and the ceramic plate were found to be of comparable magnitude and independent of the frequency of the applied field. However, the statistical scatter in the results obtained with the quartz plates was found to be about 25%. This scatter is probably due to unwanted vibrations caused by other piezoelectric coefficients which arise, in addition to d_{xxx}, from imperfect cutting and orientation of the crystal. The statistical scatter in results

when using the ceramic plate was found to be much lower. Consequently only this plate was used for subsequent measurements.

The 50 mV rms signal from the Philips wave synthesizer was externally doubled in frequency and then passed through an amplifier and phase shifter so that voltages of up to 100 V rms of any phase could be applied to the reference sample with precisely twice the frequency of the signal applied to the crystal. Voltages applied to the reference sample were measured by a Hewlett-Packard model 3478A multimeter connected across the plate. Again, as in the case of the crystal, stray fields were kept to a minimum by using short electrode connections and coaxial cables. Relative changes in the position of the reference sample and coaxial cables did not affect readings, indicating that stray fields were negligible.

3.6 FIELD-INDUCED CHANGES IN THE OPTICAL PATH LENGTH

A change in the optical path length in either arm of the interferometer leads to a shift in the phase of the emergent wave. In the following discussion separate expressions for the shift in phase resulting from the application of an electric field to the crystal and reference sample are considered.

3.6.1 Phase shift induced in the crystal

Applying a modulation voltage $V_{KDP}(\omega)$ to the crystal, through which the interferometer beam passes, leads to an alternating shift in the optical path length in that arm of the interferometer. This shift is caused by the change in refractive index Δn of the sample, due to the quadratic electro-optic effect, and a change in length ΔL due to electrostrictive dilation. The alternating change in phase of the light wave, observed at a

frequency 2ω, due to this phase retardance has an amplitude given by

$$\delta_{KDP}(2\omega) = 2k\left[L\Delta n + (n-n_1)\Delta L\right] , \qquad (3.2)$$

where $k = 2\pi/\lambda$, n_1 is the refractive index of the silicon oil surrounding the crystal, and L is the length and n the refractive index of the crystal for propagation of the light along the particular crystallographic axis of the crystal.

Chapter Two dealt with the change in refractive index as a result of the quadratic electro-optic effect and for the time being only these expressions for the field-induced changes will be considered. At this stage it is, however, important to note that other effects are also present in the physical arrangement which may contribute to the observed results. These are discussed in detail in Section 4.5.

The frequency of the field applied to the two crystals used in the experiment, typically 390 Hz, was more than two orders of magnitude lower than the frequencies of piezoresonances of the samples (Górski *et al* 1994). The crystals were therefore considered to be mechanically free. As a result the change in crystal length ΔL was attributed solely to the electrostrictive strain of the sample. The strain induced in a material due to the electrostrictive effect, which is quadratic in the applied field, is given by (see, for example, Nye 1985)

$$S_{ij} = \gamma_{klij}E_kE_l , \qquad (3.3)$$

where γ_{klij} is the fourth-rank electrostriction tensor, and $\underset{\sim}{E}$ is the applied electric field. This electric field has an amplitude given by $E = V/d$ in which V is the amplitude of the applied voltage and d is the distance between the electrodes.

The change in length ΔL_i of a crystal sample in the i^{th} direction as a result of the induced strain is given by (see, for example, Nye 1985)

$$\Delta L_i = S_{ij} L_j \ . \qquad (3.4)$$

It is the change in length of the crystal in the direction of light propagation that appears in eq. (3.2), caused by applying the field along the crystallographic x-axis. From eqs. (3.3) and (3.4) the relevant changes in the crystal length may be found, where use is made of symmetry tables given by Birss (1966):

1. For light propagation along the crystallographic z-axis

$$\Delta L_z = \gamma_{xxzz} L_z E^2 \ . \qquad (3.5)$$

2. For light propagation along the crystallographic y-axis

$$\Delta L_y = \gamma_{xxyy} L_y E^2 = \gamma_{yyxx} L_y E^2 \ . \qquad (3.6)$$

Unfortunately, the lack of electrostrictive data for KDP means that precise values for the electrostrictive contribution to δ_{KDP} cannot always be found. In an effort to reduce its contribution, the oil in the KDP bath was chosen to have a refractive index close to that of the sample: this keeps the factor $(n-n_1)$ in eq. (3.2) small. The oil used in the experiment was found to have a refractive index $n_1 = 1.5572$, which compares with the refractive indices of KDP for light polarized in the z-direction and in the y- or x-directions respectively of $n_z = n_e = 1.467$ and $n_{x,y} = n_o = 1.507$. These values are for room temperature and $\lambda = 632.8$ nm (Landolt-Börnstein 1979).

Making use of eqs. (2.41), (2.43) and (2.44), as well as the above, one may show that the total change in phase of the light wave when the field is

applied to the crystal is:

1. For light propagating along the crystallographic z-axis and linearly polarized at an angle α to the x-axis

$$\delta^{z}_{KDP} = 2kL\left[-\frac{1}{2}n_o^3\left(g_{xxxx}\cos^2\alpha + g_{yyxx}\sin^2\alpha + n_e^2[r_{yzx}]^2\sin^2\alpha\right) + (n_o-n_1)\gamma_{xxzz}\right]E^2 \quad . \quad (3.7)$$

2. For light propagating along the crystallographic y-axis and linearly polarized, in turn, along the x- and z-axes

$$\delta^{y}_{KDP} = 2kL\left[-\frac{1}{2}n_o^3 g_{xxxx} + (n_o-n_1)\gamma_{yyxx}\right]E^2 \quad , \quad (3.8)$$

$$\delta^{y}_{KDP} = 2kL\left[-\frac{1}{2}n_e^3\left(g_{zzxx} + n_o^2[r_{yzx}]^2\right) + (n_e-n_1)\gamma_{yyxx}\right]E^2 \quad . \quad (3.9)$$

3.6.2 Phase shift induced in the reference sample

In the other arm of the interferometer the alternating shift in the phase of the radiation, resulting from an alternating change in the optical path length, was a consequence of the piezoelectric effect of the ceramic reference plate. An expression analogous to that given in eq. (3.4), but now in terms of the ceramic's change in thickness, is given by

$$\Delta L = dV_{ref} \quad , \quad (3.10)$$

where d is the piezoelectric coefficient, and V_{ref} is the amplitude of the voltage applied to the plate, which produce a change in length in that direction.

The piezoelectric response of the ceramic reference plate used in this research was found experimentally to be independent of the frequency of the applied field, up to frequencies of about 2 kHz. By means of a Fluke high voltage power supply, model 412B, a dc field was applied across the ceramic

in order to determine its piezoelectric coefficient. It was found that for a dc voltage of 1030 V the change in optical path length led to a shift in phase of the interferometer beam of 180°, as read by means of the lock-in amplifier. As the interferometer beam has a wavelength of 632.8 nm, it was possible to calculate that the coefficient of the piezoelectric response of the reference sample had a magnitude of 3.07×10^{-10} mV^{-1}.

The alternating change in length of the ceramic reference sample, due to the application of a modulation voltage V_{ref}, leads to an alternating shift in the phase in radiation in that arm of the interferometer which may intuitively be seen to have an amplitude given by

$$\delta_{ref} = - 2kdV_{ref} . \qquad (3.11)$$

3.7 THE DETECTION SYSTEM

The interference pattern formed by the interferometer was focused, by means of a converging lens, on the aperture of a photodiode. This photodiode was operated at 30 V and its response to changes in light intensity was found to be linear over the range used in this investigation. Amplification of the signal was achieved by a preamplifier built into the photodiode circuitry, that could be adjusted to give ×1, ×5, ×10, or ×50 signal enhancement. The photodiode output was connected via a coaxial cable to the input of the lock-in amplifier (EG & G Princeton Applied Research model 5210). A background signal of the order of 2 μV, resulting from the laser intensity, was detected when no voltages were applied across either the reference or crystal samples.

An input signal for the lock-in amplifier reference was taken from the TTL output of the Philips wave synthesizer. Selection keys on the front panel

of the lock-in amplifier allowed for easy adjustment of all its functions. The 2F mode was selected, which meant that the reference channel operated at twice the frequency ω of the applied reference signal. This was necessary to facilitate second-harmonic measurements. The signal channel input from the photodiode could be filtered by means of a low-pass, band-pass, or notch filter tuned manually to any desired frequency, or automatically to the reference channel operating frequency. The band-pass filter was selected, automatically tuned to 2ω, which provided attenuation of the signal above and below 2ω. In addition to these filters the signal could be passed through a separate line-reject (notch) filter tuned automatically to either F or 2F. These line filters operated independently of the other filter functions. The F mode for the line-reject filter was selected in this research to provide attenuation of more than 34 dB at a stopband of ±1% at the line frequency ω. This was also necessary in order to facilitate second-harmonic measurements.

The sensitivity of the lock-in amplifier had a range of 100 nV to 3 V full scale deflection, but was typically set at 1 mV. A time constant setting of between 300 ms and 3 s was usually selected, depending on the stability, from the permitted range of 1 ms to 3 ks. The maximum dynamic reserve of the lock-in amplifier was 60 dB.

3.8 THE COMPENSATION TECHNIQUE

For the applied field and light propagation constraints considered in this investigation, the application of a voltage of frequency ω to the KDP crystal leads to an alternating phase shift of frequency 2ω of the beam passing through the crystal. This alternating phase shift was due to the quadratic electro-optic effect and electrostriction of the crystal.

Similarly, the application of a voltage of frequency 2ω across the ceramic disc resulted in an alternating phase shift of the beam in that arm of the interferometer due to the piezoelectric effect. These alternating phase shifts led to a modulation, at 2ω, of the intensity of the interference pattern incident on the photodiode.

As the lock-in amplifier was set to detect signals modulated at 2ω from the photodiode, it gave an amplitude of the total field-induced phase shift in the interferometer which was displayed on its analogue and digital outputs. A second digital display gave the phase of the alternating phase shift with respect to the phase of the reference signal.

In order to compensate for the alternating phase shift induced by applying the modulation voltage of fixed amplitude to the KDP crystal with the alternating shift produced in the ceramic reference sample, it was necessary to ensure that the two alternating shifts were 180° out of phase. This was achieved by means of the phase shifter (see Figure 3.1), which allowed the phase of the modulation voltage applied across the ceramic disc to be adjusted, which in turn shifted the phase of the retardation.

CHAPTER FOUR

EXPERIMENTAL RESULTS AND DISCUSSION

4.1 THE COMPENSATION APPROACH

One necessary test, which was conducted before measurements were made in this research, was to determine whether the magnitude of the induced change in phase of the light beam passing through the KDP crystal depended on the frequency of the modulation voltage applied to the crystal. Such a dependence should not, in principle, be observed, as the applied voltage frequencies were well below those of piezoresonances of the samples, and over the range of these frequencies the dispersion of the quadratic electro-optic coefficients is negligible. For a fixed amplitude of the voltage and for various frequencies in the range used, namely 200 to 800 Hz, no such dependence could be found.

With the modulation voltage applied across the KDP crystal, the reference and photodiode signals were brought into phase at the lock-in amplifier in order to maximize the amplifier's output. This output was then monitored as the amplitude of the alternating voltage applied to the ceramic disc was varied. When compensation between the signals in either arm of the interferometer was achieved a zero output was displayed on the lock-in amplifier, and the voltage applied to the ceramic was taken as being the compensation voltage.

When compensation was achieved the shifts in phase in either arm of the interferometer were equal in both magnitude and sign. Under these circumstances one may conclude from eqs. (3.7) to (3.9), and (3.11) that:

1. For light propagating along the crystallographic z-axis and linearly polarized at an angle α to the x-axis

$$\frac{2dV_{ref}}{n_o^3 L E_{KDP}^2} = g_{xxxx}\cos^2\alpha + g_{yyxx}\sin^2\alpha + n_e^2[r_{yzx}]^2\sin^2\alpha - 2(n_o-n_1)n_o^{-3}\gamma_{xxzz} . \quad (4.1)$$

2. For light propagating along the crystallographic y-axis and linearly polarized, in turn, along the x- and z-axes

$$\frac{2dV_{ref}}{n_o^3 L E_{KDP}^2} = g_{xxxx} - 2(n_o-n_1)n_o^{-3}\gamma_{yyxx} , \quad (4.2)$$

$$\frac{2dV_{ref}}{n_e^3 L E_{KDP}^2} = g_{zzxx} + n_o^2[r_{yzx}]^2 - 2(n_e-n_1)n_e^{-3}\gamma_{yyxx} . \quad (4.3)$$

In eqs. (4.1) to (4.3), E_{KDP} and V_{ref} are respectively the amplitudes of the modulation electric field and voltage for the KDP and reference sample when compensation is achieved. Landolt-Börnstein (1979) gives the value for the linear electro-optic coefficient which appears in eqs. (4.1) and (4.3) as -8.8×10^{-12} mV^{-1}. Consequently, the terms in these equations involving this component amount to the order of 10^{-22} m^2V^{-2} which, being two orders of magnitude smaller than the measured effect, can be neglected (Górski *et al.* 1994).

4.2 DATA COLLECTION

The longer and thinner of the two crystals available for use in the experiment produced, because of its greater optical path length, a sharper conoscopic image than the other and thus could be aligned with greater certainty. Also, as the second crystal was both thicker and shorter the changes in the optical path length it induced were smaller for the applied voltages. This meant that the photodiode output obtained with the second

crystal had a poorer signal-to-noise ratio. Accordingly, it was decided to use the longer and thinner crystal in this investigation whilst the other was used, where possible, as a check for the consistency of results.

The signs of the electro-optic coefficients measured in this experiment were determined on the basis that a positive voltage applied to the ceramic disc lead to a decrease in optical path length in that arm of the interferometer. In this way for modulation voltages of the same phase applied to the KDP and ceramic samples the phase of the induced alternating shifts of radiation in each arm of the interferometer were noted.

4.2.1 Light propagation along the crystallographic z-axis

Before proceeding with the measurements all the optical components, except the beam splitter, were aligned perpendicular to the interferometer light path. This was achieved by careful orientation of the components concerned until the beam reflected of each face retraced the path of the incident light. Care was also taken to ensure the maximum transmission of the beam through the interferometer. The crystal itself, placed in the oil bath in an arm of the interferometer, was oriented as described in Section 3.4 so that the beam was directed along its z-axis. This arrangement is depicted in Figure 4.1(a).

The compensation voltage across the reference sample was measured for voltages applied to the KDP crystal which resulted in fields in the range 2.0 to 4.0 $\times$ 10^5 Vm^{-1}, and for various angles α of linear polarization of the incident light wave, where α is the angle between the crystallographic x-axis and the direction of polarization of the light wave propagating through the crystal. This angle was varied between -90° and 90° by means of

the Glan-Taylor polarizing prism (see Figure 3.1), so covering all possible planes of linear polarization. For the incident light polarized at 0° the quadratic electro-optic coefficient responsible for the field-induced alternating phase shift is g_{xxxx}, while for light polarized at $|90^\circ|$ the coefficient is g_{yyxx}. This latter coefficient is found to be considerably smaller in magnitude and opposite in sign to the g_{xxxx}. As the angle of the incident light polarization is rotated from 0° through to $|90^\circ|$ the contribution due to the g_{xxxx} coefficient becomes less dominant and that of the g_{yyxx} coefficient more so. It was found experimentally that for angles of polarization greater than $|60^\circ|$ the signal for the induced alternating phase shift was small, strongly affected by noise, and its phase unstable. This is because for these angles the g_{yyxx} coefficient becomes the more dominant, and being small and giving rise to a signal 180° out of phase with that due to g_{xxxx}, it is difficult to obtain a sensitive and stable reading for the range of applied voltages used.

With the compensation voltages obtained, eq. (4.1) was used to determine values for $g_{xxxx}\cos^2\alpha + g_{yyxx}\sin^2\alpha - 2(n_o-n_i)n_o^{-3}\gamma_{xxzz}$ for the measured angles α. These values, denoted by the symbol r, were plotted as a function of α, as shown in the polar plot in Graph 4.1. Each point plotted on this graph corresponds to the mean of approximately 300 experimental readings. A simple least squares analysis was performed on the experimental points, where the function on the right hand side of eq. (4.1) was differentiated with respect to the parameters g_{xxxx}, g_{yyxx}, and γ_{xxzz}. The effect of the last being taken as small. In this analysis it was assumed that the uncertainty in the measured values was contained within r and that the angle α was known to a greater precision. This is a reasonable assumption since the angle of linear polarization of the light incident on the crystal

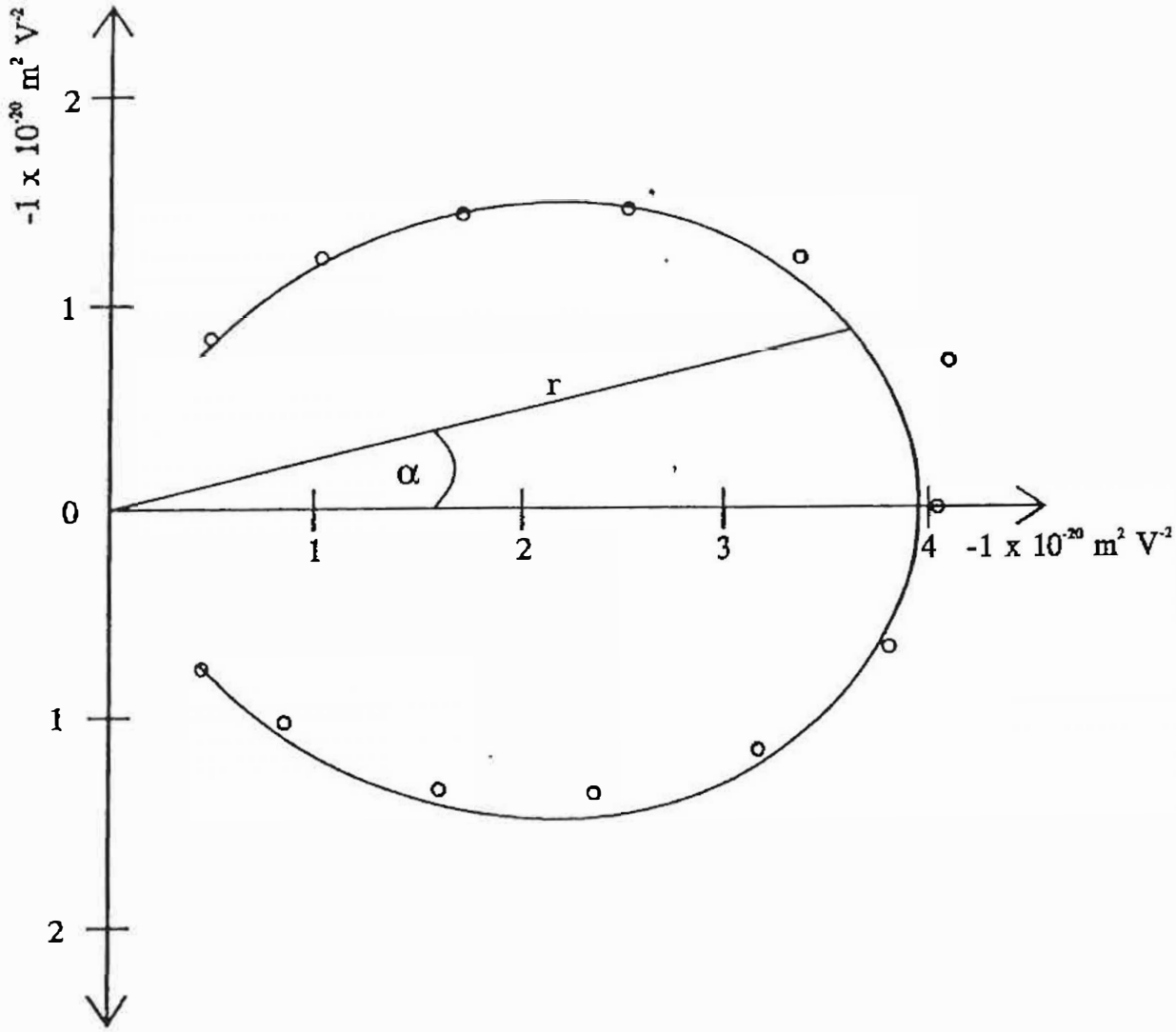

Graph 4.1 A polar plot of the values of $r = 2dV_{ref}/n_o^3 L E_{KDP}^2$ *for angles* α *of the incident light linear polarization between 60° and -60°. Also shown is the best-fit curve determined by a least squares analysis.*

could be set to within 2′ of arc by means of the divided circle bearing the Glan-Taylor prism. From this analysis results for $g_{xxxx} - 2(n_o-n_1)n_o^{-3}\gamma_{xxzz}$ and $g_{yyzz} - 2(n_o-n_1)n_o^{-3}\gamma_{xxzz}$ were determined together with their experimental uncertainty. By means of these two results it was possible to plot the best-fit curve shown in Graph 4.1, satisfying the theoretical relationship given in eq. (4.1). From the curve an indication is given of the extent to which the experimental points agree with the theory. The experimental points were found to have a standard deviation of about 6% from the best-fit curve.

From the best-fit curve the following results for $\alpha = 0^\circ$ and $|90^\circ|$ respectively were obtained:

$$g_{xxxx} - 2(n_0-n_1)n_o^{-3}\gamma_{xxzz} = -(4.0 \pm 0.5) \times 10^{-20}\ m^2V^{-2}\ , \qquad (4.4)$$

$$g_{yyxx} - 2(n_0-n_1)n_o^{-3}\gamma_{xxzz} = (0.2 \pm 0.1) \times 10^{-20}\ m^2V^{-2}\ . \qquad (4.5)$$

The second crystal, with a larger signal-to-noise ratio and being more difficult to align accurately, yielded a result only for $\alpha = 0^\circ$, which from eq. (4.1) is given by

$$g_{xxxx} - 2(n_0-n_1)n_o^{-3}\gamma_{xxzz} = -(4.4 \pm 0.7) \times 10^{-20}\ m^2V^{-2}\ . \qquad (4.6)$$

The results in eqs. (4.4) and (4.6) may be seen to agree within the limits of their experimental uncertainty.

4.2.2 Light propagation along the crystallographic y-axis

Due to the natural birefringence in KDP when light propagates off the optic axis, no relationship as shown in Graph 4.1 could be plotted for light propagating along the crystallographic y-axis.

With the optical system aligned, the beam was directed along the y-axis of the crystal as described in Section 3.4. This arrangement is shown in Figure 4.1(b). Compensation voltages were then measured for the two cases of the incident light linearly polarized in turn along the crystallographic x- and z-axes. From these compensation measurements and with the use of eqs. (4.2) and (4.3) the following results, for this light path, were obtained:

$$g_{xxxx} - 2(n_o - n_i)n_o^{-3}\gamma_{yyxx} = -(3.9 \pm 0.6) \times 10^{-20}\ m^2V^{-2}\ , \qquad (4.7)$$

$$g_{zzxx} - 2(n_e - n_i)n_e^{-3}\gamma_{yyxx} = -(0.6 \pm 0.1) \times 10^{-20}\ m^2V^{-2}\ . \qquad (4.8)$$

The close agreement of the experimental results given in eqs. (4.4) and (4.7) suggest that the values of the quadratic electrostrictive coefficients γ_{xxzz} and γ_{yyxx} are either nearly equal or that their contributions to the quadratic electro-optic terms are negligible.

4.3 EXPERIMENTAL UNCERTAINTIES

Equations (4.1) to (4.3) from which the experimental results are calculated in this research contain several variables. The uncertainties quoted in the results given in eqs. (4.4) to (4.8) take into account the uncertainties in these measured variables as well as the statistical scatter in the results obtained by compensation means. Misalignments in the angle of linear polarization of the incident light wave with respect to the crystallographic axes and the contributions due to possible fringing field effects are also discussed as possible sources of uncertainties.

4.3.1 Uncertainties in the measured variables

The dimensions of the two KDP crystal samples used in this research were measured by means of a travelling microscope which was accurate to within 0.01 mm. To obtain reliable results for the dimensions of the crystals a large number of readings was taken over the entire surfaces of both. The accuracy of the crystal dimensions measured in this way was estimated to be within 0.8%.

The compensation voltage necessary to be applied to the ceramic disc and the voltage applied to the KDP crystal were measured by means of $5\frac{1}{2}$ - digit Hewlett-Packard multimeters. These meters have a precision to within ±0.4% for the range and frequencies of the voltages being measured in this experiment. Accordingly, the error in V_{ref} was due to the uncertainty in finding the compensation position, or zero output on the lock-in amplifier, rather than the precision of the measurement of the voltage. Similarly the error in the voltage applied across the crystal was determined not by the limitations of the voltmeter but by the accuracy of the calibration technique. Section 3.4 dealt with this particular uncertainty.

The piezoelectric response of the ceramic disc, as mentioned in Section 3.6, was found by determining the magnitude of the dc voltage necessary to be applied to the it in order to result in a phase shift of 180° in the optical radiation in that arm of the interferometer. This procedure was repeated at intervals during the research and on the basis of these results it was determined that such a voltage was of the order of (1030 ± 20)V. The error in this result outweighs the uncertainty in the voltage supplied by the Fluke DC power supply, which has an accuracy specified to be better than ±0.25% of its preset value. In order to determine the piezoelectric

coefficient of the plate from this result, the wavelength of the radiation used is required. For a He-Ne laser this was taken to be 632.8 nm. The uncertainty in the ceramic plate's piezoelectric coefficient was calculated to be ±2.2%.

4.3.2 Statistical spread of the results

The results obtained for the compensation voltage applied to the ceramic disc for the various angles of incident light polarization, and for both directions of light propagation, had varying amounts of statistical scatter. For this reason a large number of readings was taken in each case and the standard error S_n in the results estimated. The standard error in a reading is given as

$$S_n = \sqrt{\frac{\sum (x_1 - \bar{x})^2}{n(n-1)}} ,$$

where $\bar{x}$ is the mean of a set of n readings of x_1.

In the cases of eqs. (4.6) to (4.8), where the results were obtained directly from measurements and not by graphical means, this standard error was included in the uncertainty in the results. In the case of the plotting of the polar plot in Graph 4.1, the standard error in the results for $g_{xxxx} - 2(n_o-n_1)n_o^{-3}\gamma_{xxzz}$ and $g_{yyxx} - 2(n_o-n_1)n_o^{-3}\gamma_{xxzz}$ was found by means of the simple least mean squares analysis, where the function to be satisfied was that given in eq. (4.1).

4.3.3 Uncertainty in the angle of linear polarization

In this research it is quite possible that the direction of 0° for the incident light's linear polarization was not exactly along the x-axis of the crystal. Consequently, it is necessary to calculate what influence

small errors $\delta\alpha$ in α would have on the experimental results.

For light propagation along the crystallographic z-axis it was possible to use the best-fit curve to calculate the magnitude of the uncertainties in the experimental results for $g_{xxxx} - 2(n_0-n_1)n_o^{-3}\gamma_{xxzz}$ and $g_{yyxx} - 2(n_0-n_1)n_o^{-3}\gamma_{xxzz}$ for errors in α up to 3°. These errors were relatively small for $g_{xxxx} - 2(n_0-n_1)n_o^{-3}\gamma_{xxzz}$ being within ±0.2%, but much larger for $g_{yyxx} - 2(n_0-n_1)n_o^{-3}\gamma_{xxzz}$ being within ±25%. The result given in eq. (4.6) was assumed to have a similar uncertainty resulting from errors in α as was the case in eq. (4.4).

To calculate the errors arising from $\delta\alpha$ for light propagation along the crystallographic y-axis, it was necessary to take readings for linear polarization of the incident beam slightly off the crystal axes. For these small angles the birefringence, and resulting ellipticity, was overlooked. From these results the uncertainties, for deviations in the angle of linear polarization of up to 3°, for the case of $g_{xxxx} - 2(n_o-n_1)n_o^{-3}\gamma_{yyxx}$ was found to be ±0.8%, and for $g_{zzxx} - 2(n_e-n_1)n_e^{-3}\gamma_{yyxx}$ was within ±6.0%.

4.3.4 Fringing fields

When a voltage is applied across the KDP crystal electrodes the field formed is not necessarily restricted directly between the plates in the sample, since it is possible for a field to exist around the crystal edges. This field is referred to as a fringing field and is depicted in Figure 4.2. It was a necessary precaution to check that this field did not induce an optical birefringence in the oil surrounding the crystal measurable at 2ω.

With this in mind two parallel steel wires 5 mm apart and of 0,31 mm diameter, which were under tension, were positioned, in the absence of the crystal, in the oil bath perpendicular to the direction of light propagation. These wires simulated the upper and lower ends of the electrodes in the entrance and exit faces of the crystal. The light beam passed between the wires to which an ac voltage from the high-voltage amplifier was applied. These wires produced a field in the silicon oil which, in part, simulated the fringing field around the edges of the thinner crystal used in the final measurements, and also polarized the oil directly between the wires. As a result, any effect induced in this manner would have to be larger than that induced in the oil by the fringing field around the edge of the crystal.

It was found that these parallel wires did in fact induce an effect detectable at 2ω. As this was very small it was subject to a high signal-to-noise ratio and only a maximum value for its contribution could be estimated. No dependence on the angle of light polarization could be detected. The measurable effect induced in such a manner was included as an uncertainty in the final results.

On determining a magnitude of this effect it was possible to conclude that it contributed the following uncertainties:

$$\pm 0.5\% \text{ to } g_{xxxx} - 2(n_0-n_1)n_o^{-3}\gamma_{xxzz}$$

$$\pm 0.5\% \text{ to } g_{xxxx} - 2(n_0-n_1)n_o^{-3}\gamma_{yyxx}$$

$$\pm 10\% \text{ to } g_{yyxx} - 2(n_0-n_1)n_o^{-3}\gamma_{xxzz}$$

$$\pm 3.3\% \text{ to } g_{zzxx} - 2(n_e-n_1)n_e^{-3}\gamma_{yyxx}$$

4.4 ELECTROSTRICTIVE CONTRIBUTION TO THE PHASE SHIFT

Equations (4.1) to (4.3) contain two electrostrictive coefficients: γ_{yyxx} and γ_{xxzz}. In order to determine the magnitudes of the quadratic electro-optic coefficients contained within these equations, it is necessary to evaluate the electrostrictive terms. Only two electrostrictive coefficients for KDP have, as yet, been evaluated. These coefficients designated Q_{zzzz} and Q_{xxzz}, which are specified in terms of the polarization rather than applied field, have been determined accurately by means of a neutron and gamma ray diffraction technique, in which changes in the lattice constants of KDP at low temperature were induced by an applied field (Troussant *et al.* 1988). These values are given as

$$Q_{zzzz} = (2.95 \pm 0.02) \times 10^{-1}\ \mathrm{m^4C^{-2}}\ ,$$

$$Q_{xxzz} = (2.74 \pm 0.04) \times 10^{-1}\ \mathrm{m^4C^{-2}}\ ,$$

and are known to be weakly dependent on temperature in the paraelectric phase.

From Kaminow (1974) the coefficients Q_{ijij} and γ_{ijij} are related by

$$\gamma_{ijij} = \varepsilon_o^2(\varepsilon_j(0)-1)^2 Q_{ijij}\ . \qquad (4.9)$$

where ε_o is the permittivity of free space and $\varepsilon_j(0)$ is the diagonal component of the low-field dielectric constant, with the same understanding of repeated subscripts as in eqs. (2.39) and (2.40). One finds, by means of eq. (4.9), that for KDP at room temperature

$$\gamma_{zzzz} \approx 0.9 \times 10^{-20}\ \mathrm{m^2V^{-2}}\ ,$$

$$\gamma_{xxzz} \approx 0.8 \times 10^{-20}\ \mathrm{m^2V^{-2}}\ .$$

These results suggest that the electrostrictive coefficients of KDP that enter eqs. (4.1) to (4.3) are of the order of magnitude of $10^{-20}\ \mathrm{m^2V^{-2}}$. From this deduction, and the values $2(n_o-n_1)n_o^{-3} = 0.029$ and $2(n_e-n_1)n_e^{-3} =$

-0.055, the electrostrictive contribution in these equations may be seen to be small and the measured results due mainly to the quadratic electro-optic effect. If one assumes that the absolute values of the electrostrictive coefficients for KDP are no greater than 5×10^{-20} m^2V^{-2}, and including the electrostrictive contributions as an uncertainty in the measured effect, then the results for the quadratic electro-optic coefficients of KDP obtained in this experiment may be given as

$$g_{xxxx} = -(4.0 \pm 0.6) \times 10^{-20} \ m^2V^{-2} ,$$

$$g_{yyxx} = g_{xxyy} = (0.2 \pm 0.2) \times 10^{-20} \ m^2V^{-2} ,$$

$$g_{zzxx} = g_{zzyy} = -(0.6 \pm 0.3) \times 10^{-20} \ m^2V^{-2} .$$

4.5 PHYSICAL COMPONENTS OF THE OBSERVED QUADRATIC EFFECT

In an experiment such as the one conducted in this investigation the field-induced change in the refractive index is due not only to the electro-optic effect, but also to the stress induced in the crystal due to the electrostatic attraction of the electrodes. Under these conditions an expression for the electric field-induced change in the refractive index due to the quadratic electro-optic effect may be given by (see, for example, Bohatý and Haussühl 1977):

$$\Delta\eta_{\alpha\beta} = g_{\alpha\beta\gamma\delta}E_\gamma E_\delta + q_{\alpha\beta\gamma\delta}\sigma_{\gamma\delta} , \qquad (4.10)$$

where $g_{\alpha\beta\gamma\delta}$ is the quadratic electro-optic tensor component, and $q_{\alpha\beta\gamma\delta}$ and $\sigma_{\gamma\delta}$ are respectively components of the piezo-optic and the mechanical stress tensors.

The measurements in this experiment were carried out with a field applied to the crystal which was modulated at a frequency well below its fundamental piezoresonance frequencies. In these circumstances the crystal is free to deform and the applied field will induce strains in the material

through the piezoelectric and electrostrictive effects, where the variation in the strain follows the modulation field. As the crystal is free to respond, it is by convention considered to be unclamped and the quadratic electro-optic coefficient measured under these conditions is designated $g_{\alpha\beta\gamma\delta}$ (constant stress).

If the field applied to the crystal were modulated at a frequency well above the fundamental piezoresonance frequencies, the crystal would not deform, in which case it is considered to be clamped. The quadratic electro-optic coefficient obtained under these conditions is called the primary (or true) coefficient, and is designated $\bar{g}_{\alpha\beta\gamma\delta}$ (constant strain).

Because their measurement conditions are not the same, the electro-optic coefficient $g_{\alpha\beta\gamma\delta}$, measured in this experiment, differs from $\bar{g}_{\alpha\beta\gamma\delta}$ by (see, for example, Kaminow 1974)

$$g_{\alpha\beta\gamma\delta} - \bar{g}_{\alpha\beta\gamma\delta} = p_{\alpha\beta\varepsilon\lambda}\gamma_{\gamma\delta\varepsilon\lambda} \ , \qquad (4.11)$$

where $p_{\alpha\beta\varepsilon\lambda}$ and $\gamma_{\gamma\delta\varepsilon\lambda}$ are the elasto-optic and quadratic electrostrictive coefficients respectively. The term on the right hand side of eq. (4.11) describes the elasto-optic-electrostrictive contribution to the quadratic electro-optic effect.

In this experiment the crystal was mounted in such a way to allow strains to take place as freely as possible and under these conditions eq. (4.11) holds.

The electro-optic coefficient $g_{\alpha\beta\gamma\delta}$ measured in this experiment may be related to the primary quadratic electro-optic coefficient, the elasto-optic-electrostrictive contribution, and the term resulting from the

piezo-optic effect and the stress due to the attraction of the electrodes by (see, for example, Górski *et al.* 1994)

$$g_{\alpha\beta\gamma\delta}E_\gamma E_\delta = \bar{g}_{\alpha\beta\gamma\delta}E_\gamma E_\delta + p_{\alpha\gamma\epsilon\lambda}\gamma_{\gamma\delta\epsilon\lambda}E_\gamma E_\delta + q_{\alpha\beta\gamma\delta}\sigma_{\gamma\delta} \ . \qquad (4.12)$$

4.6 DISCUSSION OF RESULTS

Table 4.1 shows experimental results for the quadratic electro-optic coefficients of KDP which have been published previously, as well as those obtained in this research. Past methods of measurement involved using static and dynamic polarimetric approaches, with the notable exception of the value $g_{zzzz} < 2.4 \times 10^{-21}\ m^2V^{-2}$, which was estimated for KDP by electro-optic deflection techniques (Grib *et al.* 1975). Comparison of the results obtained in this experiment with the published ones shows that the magnitudes of results from this work are comparable to those obtained by the dynamic polarimetric method (Górski & Kucharczyk 1987; Jamroz & Karniewicz 1979) and by Grib *et al.* (1975), but are two orders of magnitude smaller than those obtained employing the static technique (Perfilova & Sonin 1967; Jamroz *et al.* 1979).

For the directions of the applied field and light path used in this experiment the linear electro-optic effect is, in principle, non-existent and the quadratic response becomes the leading effect. However, it must be noted that factors such as the imperfect cutting of the crystal, inaccuracies in crystal alignment, and to a certain extent the angular divergence of the laser beam lead to changes in the considered constraints. Also, KDP is known to exhibit a large piezoelectric effect which can lead to vibrations of the sample and deviate the light beam from the desired direction of propagation (Kucharczyk 1992).

Kucharczyk and Górski (1983) performed a numerical estimation, neglecting the effect of the quadratic coefficients, of a possible dependence, through the linear electro-optic coefficients, on the square of the applied field of the induced birefringence of a KDP crystal for slight angular deviations of the light wave propagation and applied field directions. The divergence of the laser beam was not considered. They concluded that in some particular cases a linear or near linear dependence on the square of the applied field of the induced birefringence is brought about by the linear electro-optic effect, and that it was perhaps this dependence which lead to the larger results estimated by the static polarimetric techniques. It is evident that while interpreting results for KDP in these configurations, possible contributions from the linear electro-optic effect should be recognized.

In this experiment the importance of relating the phase modulation observed in the KDP unambiguously to the quadratic electro-optic effect was appreciated. For light propagating along the optic axis of KDP, to which a low-frequency electric field is applied in the crystallographic x-direction, the induced electro-optic effect quadratic in the applied field, for which the coefficients g_{xxxx} and g_{yyxx} are responsible, should satisfy the relation given in eq. (4.1). Checking whether the experimentally observed effect quadratic in the applied field transforms according to this relationship provides confirmation that the observed effect is indeed related to these coefficients. Accordingly, for light propagation along the optic axis, the dependence of the induced electro-optic effect on the angle of incident light polarization, was checked. From Graph 4.1 it may clearly be seen that a satisfactory agreement between the experimental results and the theoretical dependence

was obtained. It may be concluded that in this experiment contributions due to lower-order effects did not lead to any significant influence.

4.7 BOND-POLARIZABILITY MODEL

The bond-polarizability model is one of several theoretical approaches that has been invoked in the past to discuss electro-optic effects of KDP-type crystals. This theoretical study of the electro-optic effect was developed by Shih and Yariv (1980, 1982) based on the single-energy-gap model (Penn 1962) applied to a dielectric by Phillips and Van Vechten (1969), and also on the bond-charge calculation of bond non-linearity (Levine 1973a, b). It takes into account the dependence of the crystal's optical susceptibility on the bond-rotation and bond-stretch induced by the applied low-frequency electric field. From this relation an expression for the electro-optic coefficient of the crystal can be derived.

In their papers Shih and Yariv (1980, 1982) derive a general expression for the linear electro-optic coefficient of crystals, which they then apply to a wide range of samples, including KDP. Their theoretical results are found to be in very good agreement with those obtained experimentally. Kucharczyk (1987) extended their approach in order to derive an expression for the ionic contribution to the quadratic electro-optic coefficient of LiF, and in a later paper (Kucharczyk 1992) considered the quadratic effect in KDP. In the following discussion the bond-polarizability model of the electro-optic effect in KDP, as proposed by Shih and Yariv (1980, 1982) and extended by Kucharczyk (1987, 1992), is briefly reviewed so that the results obtained in this research may be considered in the context of this approach. This method will enable us, by means of the value $g_{xxxx} - g_{yyxx}$ determined in this experiment, to evaluate the ionic parts of the primary

quadratic electro-optic coefficients $\bar{g}_{xxxx}$, $\bar{g}_{yyxx}$, and $\bar{g}_{zzxx}$ for KDP.

The term in eqs. (4.4) and (4.5) which arises from the electrostrictively-induced change in path length, as shown eqs. (3.5) and (3.6), cancels when the relative value of $g_{xxxx} - g_{yyxx}$ is found. It is evident from eq. (4.12) that the quantity $g_{xxxx} - g_{yyxx}$ measured in this investigation differs from $\bar{g}_{xxxx} - \bar{g}_{yyxx}$ by the elasto-optic-electrostrictive and the piezo-optic and mechanical stress components. However, for the symmetry point group $\bar{4}2m$, to which KDP belongs, the symmetry restrictions imposed on the elasto-optic and electrostrictive tensors (Birss 1966) reduce the combined elasto-optic-electrostrictive contribution to the term $(p_{xxxx} - p_{yyxx})(\gamma_{xxxx} - \gamma_{yyxx})$. Knowledge of the elasto-optic coefficients of KDP from Landolt-Börnstein (1979), namely $p_{xxxx} - p_{yyxx} = 0.002$, along with the predictions made previously for the magnitude of the electrostrictive coefficients of KDP, suggests that the combined contribution to $\bar{g}_{xxxx} - \bar{g}_{yyxx}$ due to the elasto-optic-electrostrictive coefficients is of the order of 10^{-22} m^2V^{-2}, which is at least two orders of magnitude smaller than the measured effect.

Similarly, an estimation of the magnitude of the piezo-optic and mechanical stress contribution may be made from the values of the piezo-optic coefficients of KDP from Landolt-Börnstein (1979), and also from the equation for the induced mechanical stress σ for the field applied along the crystallographic x-axis (Haussühl & Weber 1977)

$$\sigma_{xx} = -\frac{1}{2}\varepsilon_o\varepsilon_1(0)E^2 \ . \qquad (4.13)$$

Calculations show that the total piezo-optic and mechanical stress contribution is similarly two orders of magnitude smaller than the measured

effect. As a consequence of these deductions, the following approximation may be made:

$$g_{xxxx} - g_{yyxx} \simeq \bar{g}_{xxxx} - \bar{g}_{yyxx} \,. \tag{4.14}$$

Kaminow and Johnston (1967, 1969) showed that the primary electro-optic effects may be explained in terms of two types of microscopic interaction: the first being regarded as a purely electronic (or non-lattice) contribution, and the second an ionic (or lattice) contribution. Accordingly, the primary quadratic electro-optic effect may be expressed in terms of its purely electronic and ionic parts as

$$\bar{g}_{\alpha\beta\gamma\delta} = \bar{g}^{elec}_{\alpha\beta\gamma\delta} + \bar{g}^{ion}_{\alpha\beta\gamma\delta} \,. \tag{4.15}$$

The electronic contribution arises from the applied electric field directly modifying the electronic susceptibility (or refractive index) in the absence of lattice displacements, while the ionic contribution is a result of the applied field producing a lattice displacement which in turn modifies the electronic susceptibility. Because of the high frequencies in the optical regime, where the ionic motion is unable to follow the field reversals, it is only the electronic contribution to the electro-optic effect which accounts for such phenomena as harmonic generation and usually optical-mixing. It has been shown that the magnitude of the electronic contribution to the quadratic electro-optic coefficients for KDP can be obtained from wave-mixing measurements on this crystal.

Yariv and Yeh (1984) derive an expression for the electronic part of the primary quadratic electro-optic coefficient in terms of the third-order optical susceptibility $\chi^{(3)E}_{ijkl}$ as

$$\bar{g}^{elec}_{ijkl} = - \frac{12\,\chi^{(3)E}_{ijkl}}{(n^2)_{ii}(n^2)_{jj}} , \qquad (4.16)$$

where the notation $(n^2)_{ii}$ is explained in eq. (1.3). From the values of $\chi^{(3)E}_{xxxx}$ and $\chi^{(3)E}_{yyxx}$ determined for KDP by means of wave-mixing experiments (Levenson & Bloembergen 1974; Eichler *et al.* 1977), it follows that the electronic contribution to the difference of $\bar{g}_{xxxx} - \bar{g}_{yyxx}$ is of comparable magnitude to the elasto-optic-electrostrictive and piezo-optic and mechanical stress contributions, and can likewise be neglected.

Shih and Yariv (1982) express the macroscopic susceptibility of a crystal, in the bond-polarizability model, as

$$\chi_{\alpha\beta} = \frac{1}{V} \sum_n \beta_n \alpha_{n\alpha} \alpha_{n\beta} , \qquad (4.17)$$

where $\alpha_{n\alpha}$ is the relevant direction cosine, β_n is the bond polarizability along the bond direction, and the summation is taken over all bonds contained within the unit cell of volume V. This equation incorporates the assumption that the total of the susceptibilities of the individual bonds leads to the bulk susceptibility of a crystal.

It is known that three bonds exist in the KDP crystal. These are: H-O, K-O, and P-O. Levine (1973b) argues that in the paraelectric phase of KDP only the P-O bond will contribute to the observed non-linear susceptibility. Due to its high ionicity the K-O bond is considered to contribute a negligible amount (Shih & Yariv 1982), and the H-O bonds, owing to their isotropic distribution, tend to cancel each other in their contribution to the second-order non-linear susceptibility and are of small magnitude in the third-order susceptibility (Kucharczyk 1992).

Previous treatments of second-harmonic generation (Levine 1973b) and the

linear electro-optic effect (Shih & Yariv 1982) of KDP have, when the transverse component of the P-O bond susceptibility is neglected, yielded theoretical results in good agreement with those obtained experimentally. The following theoretical discussion is carried out under the assumption that all non-linearity in KDP resides in the P-O bond, and it is only the longitudinal component of this bond that need be considered.

By means of the bond-polarizability approach Kucharczyk (1987, 1992) derives an expression for the ionic contribution to the primary quadratic electro-optic coefficient of a crystal. For KDP this expression is

$$\begin{aligned}\bar{g}^{ion}_{\alpha\beta\gamma\delta}E_\gamma E_\delta = -\frac{1}{R^2 n^4 V}\times\Bigg\{\sum_n\Bigg\{\beta_n(P\text{-}O)\left(F-2f+1\right)\alpha_{n\alpha}\alpha_{n\beta}\alpha_{n\gamma}\alpha_{n\delta}+\frac{R^2}{2}\Bigg[\alpha_{n\beta}\frac{\partial^2\alpha_{n\alpha}}{\partial Q_\gamma\partial Q_\delta}\\ +\alpha_{n\alpha}\frac{\partial^2\alpha_{n\beta}}{\partial Q_\gamma\partial Q_\delta}\Bigg]+\frac{f-1}{2}\Bigg[\alpha_{n\gamma}\left(\delta_{\beta\delta}\alpha_{n\alpha}+\delta_{\alpha\delta}\alpha_{n\beta}\right)+\alpha_{n\delta}\left(\delta_{\beta\gamma}\alpha_{n\alpha}\\ +\delta_{\alpha\gamma}\alpha_{n\beta}\right)\Bigg]+\frac{1}{2}\left(\delta_{\beta\gamma}\delta_{\alpha\delta}+\delta_{\alpha\gamma}\delta_{\beta\delta}\right)\Bigg\}\times Q_\gamma Q_\delta\\ +\beta_n(P\text{-}O)f_c\Bigg\{\left(f-1/2\right)\alpha_{n\alpha}\alpha_{n\beta}\alpha_{n\gamma}\alpha_{n\delta}+\alpha_{n\delta}\left(\alpha_{n\beta}\delta_{\alpha\gamma}+\alpha_{n\alpha}\delta_{\beta\gamma}\right.\\ \left.-2\alpha_{n\alpha}\alpha_{n\beta}\alpha_{n\gamma}\right)\Bigg\}\times Q_\gamma E_\delta\Bigg\},\end{aligned} \tag{4.18}$$

where R is the bond length, Q_γ is the relative shift of the ions induced by the low-frequency electric field applied to the crystal, and $\beta(P\text{-}O)$ is the polarizability of the longitudinal component of the P-O bond. The terms f and F describe changes in the bond polarizability caused by the variations in bond length, and are given by the equations

$$f = \frac{R}{\beta(P\text{-}O)}\left(\frac{\partial\beta(P\text{-}O)}{\partial R}\right),$$

$$F = \frac{R^2}{2\beta(P\text{-}O)}\left(\frac{\partial\beta^2(P\text{-}O)}{\partial R^2}\right).$$

A displacement of the bond charge leads to a change in the bond

polarizability. When the lattice is fixed, the factor f_c is related to this change by

$$f_c = \frac{R}{\beta(P\text{-}O)}\left[\frac{\partial\beta(P\text{-}O)}{\partial E}\right] .$$

In their paper Yariv and Yeh (1982) give the relative displacement of the ions in terms of the Szigeti effective charge e_s as

$$Q_\alpha = \frac{3E_\alpha\varepsilon_o[\varepsilon(o) - \varepsilon(\infty)]\varepsilon(\infty)}{e_s[\varepsilon(\infty) + 2]N_1} , \qquad (4.19)$$

where N_1 is the density of pairs of ions, $\varepsilon(o)$ and $\varepsilon(\infty)$ are respectively the static dielectric constant and the low-frequency electronic dielectric constant, and E_k represents the applied low-frequency field in the k^{th} direction.

$\beta(P\text{-}O)$ can be expressed in terms of the total macroscopic susceptibility of KDP $\chi(P\text{-}O)$, using eq. (4.17), as

$$\beta(P\text{-}O) \approx \chi(P\text{-}O)\sum\alpha_x^2/V , \qquad (4.20)$$

Accordingly, by means of the equation (Levine 1973b)

$$d_{yzx}^{2\omega} = \left[\beta(P\text{-}O)f_c/RV\right]\sum\alpha_y\alpha_z\alpha_x , \qquad (4.21)$$

values of $d_{yzx}^{2\omega} = 0.63 \times 10^{-12}$ mV^{-1} (Landolt-Börnstein 1979), $\chi(P\text{-}O) \approx 0.85$ (Shih & Yariv 1982), and the direction cosines for KDP (Nankano *et al.* 1973) may be used to yield an order of magnitude for f_c/R for KDP of 10^{-12} mV^{-1} (Kucharczyk 1992). Similarly Kucharczyk (1992) estimated values for the Szigeti effective charge to obtain a magnitude for Q/R of 10^{-10} m^2V^{-2}. These two estimates indicate that the order of magnitude of the last contribution on the right-hand side of eq. (4.18) is about 10^{-22} m^2V^{-2} which, being two orders of magnitude smaller than the measured coefficients, can be neglected (Kucharczyk 1992).

Taking this assumption into account one can simplify the expression in eq. (4.18) for the ionic contributions to the quadratic electro-optic effect. For the coefficients considered in this research:

$$\bar{g}^{ion}_{xxxx} = \left\{ (F - 2f + 4)\alpha_x^4 + (2f - 5)\alpha_x^2 + 1 \right\} \times K \,, \tag{4.22}$$

$$\bar{g}^{ion}_{yyxx} = \left\{ (F - 2f + 4)\alpha_x^2\alpha_y^2 - \alpha_x^2 \right\} \times K \,, \tag{4.23}$$

$$\bar{g}^{ion}_{zzxx} = \left\{ (F - 2f + 4)\alpha_x^2\alpha_z^2 - \alpha_z^2 \right\} \times K \,, \tag{4.24}$$

where K is defined as

$$KE_\alpha = - \frac{\beta(P-0)Q_\alpha}{VR^2 n^4} \,.$$

In the derivation of the above equations it was necessary to use the following relationships (Kucharczyk 1987)

$$\frac{\partial^2 \alpha_{n\alpha}}{\partial Q_\alpha^2} = \frac{3\alpha_{n\alpha}(\alpha_{n\alpha}^2 - 1)}{R^2} \,,$$

$$\frac{\partial^2 \alpha_{n\alpha}}{\partial Q_\beta^2} = \frac{\alpha_{n\alpha}(3\alpha_{n\beta}^2 - 1)}{R^2} \,.$$

An equation, analogous to eq. (4.16), from Yariv & Yeh (1984) gives

$$\bar{r}^{elec}_{yzx} = - \frac{4d^{2\omega}_{yzx}}{n^4} \,. \tag{4.25}$$

Consequently, by means of the relation

$$\bar{r}_{yzx} = \bar{r}^{elec}_{yzx} + \bar{r}^{ion}_{yzx}$$

and the values of $\bar{r}_{yzx} = - 8.8 \times 10^{-12}$ mV^{-1} and $d^{2\omega}_{yzx} = - 0.63 \times 10^{-12}$ mV^{-1} given by Landolt-Börnstein (1979), $\bar{r}^{ion}_{yzx}$ may be evaluated to be $- 8.3 \times 10^{-12}$ mV^{-1}. From this result for $\bar{r}^{ion}_{yzx}$, the factor f may be evaluated by means of the expression for the ionic contribution to the linear

electro-optic coefficient given by (Shih & Yariv 1982; Kucharczyk 1992) as

$$\bar{r}^{ion}_{yzx} = - \frac{\chi(P-O)Q(f-2)\sum\alpha_x\alpha_y\alpha_z}{Rn^4 \sum\alpha_x^2} , \qquad (4.26)$$

where the values for the direction cosines of the P-O bonds and the bond lengths for KDP are taken from Nankano *et al.* (1973). This calculation yields the value $f = 2.475$.

Equations (4.22) and (4.23) lead to

$$\bar{g}_{xxxx} - \bar{g}_{yyxx} = \left\{ \left(F - 2f + 4\right)\left(\alpha_x^4 - \alpha_x^2\alpha_y^2\right) + \left(2f - 4\right)\alpha_x^2 + 1 \right\} \times K \qquad (4.27)$$

From the results for $\bar{g}_{xxxx} - \bar{g}_{yyxx}$ obtained in this investigation and the calculated value of f, eq. (4.27) may be used to obtain the value $F = 10.57$. Using these values for f and F in eqs. (4.22) to (4.24), one then calculates

$$\bar{g}^{ion}_{xxxx} = - 5.09 \times 10^{-20} \ m^2V^{-2} ,$$

$$\bar{g}^{ion}_{yyxx} = - 0.89 \times 10^{-20} \ m^2V^{-2} ,$$

$$\bar{g}^{ion}_{zzxx} = - 1.68 \times 10^{-20} \ m^2V^{-2} .$$

These results agree well with the results obtained experimentally where the elasto-optic-electrostrictive components contributing to the observed quadratic electro-optic effect are taken to be of the order 1×10^{-20} m^2V^{-2}, and the electronic contribution is assumed to be negligible.

CHAPTER FIVE

CONCLUSION AND FUTURE POSSIBILITIES

In this thesis the quadratic electro-optic effect observed in KDP was fully accounted for by an eigenvalue theory of wave propagation (Graham & Raab 1990) which consistently allows for induced electric dipoles. By means of a quantitative theory in terms of multipole property tensors of a crystal, the polarization eigenvectors were determined, and expressions derived for their refractive indices, for the specific wave propagation and applied field directions used in the present work. In this investigation the light propagation directions were taken to be along the crystallographic y- and z-axes of the non-centrosymmetric KDP crystal to which an electric field was applied in the x-direction. This allowed the quadratic effect to be determined in the absence of a linear electro-optic effect, which is non-existent for the configurations considered.

The method of measurement proposed in this experiment consisted of using a vibrating-mirror Michelson interferometer to perform a simple and rapid, yet sensitive, determination of the quadratic electro-optic coefficients g_{xxxx}, g_{yyxx}, and g_{zzxx} of KDP by phase compensation means. The experimental technique permitted the absolute determination of certain quadratic electro-optic coefficients of KDP to be made. The sign and magnitude of the relevant coefficients were found to be:

$$g_{xxxx} = -(4.0 \pm 0.6) \times 10^{-20}\ m^2V^{-2}\ ,$$

$$g_{yyxx} = (0.2 \pm 0.2) \times 10^{-20}\ m^2V^{-2}\ ,$$

$$g_{zzxx} = -(0.6 \pm 0.3) \times 10^{-20}\ m^2V^{-2}\ .$$

Previous methods of measurement for the relative quadratic electro-optic coefficients of KDP by static polarimetric means yield values two orders of

magnitude greater than those found in this work. However, the magnitude of our results are in agreement with those for the relative quadratic electro-optic coefficients that were found by a dynamic polarimetric technique and also from a diffraction experiment. The findings of this research lend support to the argument by Kucharczyk (1992) that values for the non-linear electro-optic coefficients of KDP determined by static means are overestimated.

Finally, the results of this experiment were discussed in the context of a bond-polarizability approach (Shih & Yariv 1980, 1982; Kucharczyk 1990, 1992), and values for the ionic part of the primary quadratic electro-optic coefficients calculated.

The literature on the quadratic electro-optic effect of crystalline ammonium dihydrogen phosphate (ADP), which belongs to the KDP-type family in that it has the same point group symmetry, shows a similar inconsistency to KDP in the values of the relevant coefficients obtained by static and dynamic polarimetric methods. Using a dynamic technique Górski and Kucharczyk (1987) found the value of the coefficient $|g_{xxxx} - g_{yyxx}|$ for ADP to be 4.7×10^{-20} m^2V^{-2}, whilst the results obtained for the same coefficients by the static means are at least an order of magnitude greater (Perfilova & Sonin 1967; Lomova & Sonin 1968). The smaller magnitude is within the sensitivity of our apparatus and future investigations of the quadratic electro-optic effect in ADP is a viable prospect.

Jones (1948) predicted the existence of a linear birefringence which for particular systems may exist simultaneously with the normal linear birefringence, the difference being that its fast and slow axes are

oriented at 45° to those of the normal birefringence. To the best of our knowledge no measurement of such a birefringence has, as yet, been made. However, van Staden (1993), predicts that for light propagating along the optic axis of crystals belonging to the symmetry point groups $\bar{4}$ and $\bar{6}$, and for particular directions of the applied electric field, a Jones birefringence linear in the applied field will co-exist with the normal Pockels birefringence. Furthermore, in both these symmetry point groups, the two types of birefringence are accounted for by different components of the non-linear hyperpolarizability tensor $\beta_{\alpha\beta\gamma}$. From the known range in the order of magnitude of Pockels coefficients, these two birefringences ought to be measurable by means of our experimental method, the problem remaining being to distinguish them.

APPENDIX A

RELATION BETWEEN THE HYPERPOLARIZABILITY TENSORS $\beta_{\alpha\beta\gamma}$ AND $\gamma_{\alpha\beta\gamma\delta}$ AND THE ELECTRO-OPTIC CONSTANTS $r_{\alpha\beta\gamma}$ AND $g_{\alpha\beta\gamma\delta}$.

Within the electric dipole approximation the polarization density induced in a non-magnetic source-free medium by a monochromatic plane light wave, in the presence of an applied electric field $\underset{\sim}{E}$, is given by

$$P_\alpha = \alpha_{\alpha\beta}\mathcal{E}_\beta + \tfrac{1}{2}\beta_{\alpha\beta\gamma}\mathcal{E}_\beta E_\gamma + \tfrac{1}{6}\gamma_{\alpha\beta\gamma\delta}\mathcal{E}_\beta E_\gamma E_\delta + \ldots , \tag{A.1}$$

where $\underset{\sim}{\mathcal{E}}$ is the electric field of the wave. Considering $\underset{\sim}{D}$ in the presence of an applied field one may write, to the order of electric dipoles,

$$D_\alpha = \left(\varepsilon_{\alpha\beta} + \Delta\varepsilon_{\alpha\beta}\right)\mathcal{E}_\beta . \tag{A.2}$$

In the above equation

$$\varepsilon_{\alpha\beta} = \varepsilon_o\left(\delta_{\alpha\beta} + \tfrac{1}{\varepsilon_o}\alpha_{\alpha\beta}\right) , \tag{A.3}$$

and

$$\Delta\varepsilon_{\alpha\beta} = \tfrac{1}{2}\beta_{\alpha\beta\gamma}E_\gamma + \tfrac{1}{6}\gamma_{\alpha\beta\gamma\delta}E_\gamma E_\delta , \tag{A.4}$$

where terms of third- and higher-order in the applied field have been neglected.

Defining the electric field-induced changes to the impermeability tensor in terms of the electro-optic constants gives:

$$\eta_{\alpha\beta}(\underset{\sim}{E}) - \eta_{\alpha\beta}(0) \equiv \Delta\eta_{\alpha\beta} = r_{\alpha\beta\gamma}E_\gamma + g_{\alpha\beta\gamma\delta}E_\gamma E_\delta . \tag{A.5}$$

From the definition of the impermeability tensor, eq. (1.10), it follows that

$$\eta_{\alpha\beta} + \Delta\eta_{\alpha\beta} = \frac{\varepsilon_o}{\varepsilon_{\alpha\beta} + \Delta\varepsilon_{\alpha\beta}} . \tag{A.6}$$

This may be written in subscript (but not a tensor) notation as

$$\eta_{ij} + \Delta\eta_{ij} = \frac{\varepsilon_o}{\varepsilon_{ij}(1 + \Delta\varepsilon_{ij}/\varepsilon_{ij})}$$

$$= \frac{\varepsilon_o}{\varepsilon_{ij}} - \frac{\varepsilon_o \Delta\varepsilon_{ij}}{\varepsilon_{ij}\varepsilon_{ij}} ,$$

therefore

$$\Delta\eta_{ij} = - \frac{\varepsilon_o \Delta\varepsilon_{ij}}{\varepsilon_{ij}\varepsilon_{ij}} . \qquad (A.7)$$

Assuming that $\varepsilon_{ij}\varepsilon_{ij} \approx \varepsilon_{ii}\varepsilon_{jj}$ as implied by Yariv & Yeh (1984), and using eqs. (A.4) and (A.5), one may write

$$r_{ij\alpha}E_\alpha + g_{ij\alpha\beta}E_\alpha E_\beta = - \frac{\varepsilon_o \beta_{ij\alpha}E_\alpha}{\varepsilon_{ii}\varepsilon_{ij}} - \frac{\varepsilon_o \gamma_{ij\alpha\beta}E_\alpha E_\beta}{\varepsilon_{ii}\varepsilon_{jj}} . \qquad (A.8)$$

Thus

$$\frac{1}{2\varepsilon_o}\beta_{ijk} = - n_i^2 n_j^2 r_{ijk} , \qquad (A.9)$$

$$\frac{1}{6\varepsilon_o}\gamma_{ijkl} = - n_i^2 n_j^2 g_{ijkl} , \qquad (A.10)$$

where the expression for the principal indices of refraction is given as $n_i^2 \equiv \varepsilon_{ii}/\varepsilon_o$, and summation over the indices is not implied.

REFERENCES

Barker, A.S. & Loudon, R. 1972 *Rev. Mod. Phys.* **44**, 18.

Barron, L.D. & Buckingham, A.D. 1971 *Molec. Phys.* **20**, 1111.

Barron, L.D. & Gray, C.G. 1973 *J. Phys.* A **6**, 59.

Birss, R.R. 1966 *Symmetry and Magnetism.* Amsterdam: North-Holland.

Born, M. 1918 *Ann. Physik.* **55**, 177.

Born, M. & Wolf, E. 1980 *Principles of Optics.* Oxford: Pergamon Press.

Bohatý, L. & Haussühl, S. 1977 *Acta. Crysta.* A **33**, 114.

Buckingham, A.D. 1967 *Adv. Chem. Phys.* **12**, 107.

Buckingham, A.D. & Dunn, M.B. 1971 *J. Chem. Soc.* A, 1988.

Buckingham, A.D. & Pople, J.A. 1955 *Proc. Phys. Soc.* A **68**, 905.

Buckingham, A.D. & Stephens, P.J. 1966 *Rev. Phys. Chem.* **17**, 399.

de Figueiredo, I.M.B. & Raab, R.E. 1981 *Proc. R. Soc. Lond.* A **375**, 425.

Eichler, H.J., Fery, H., Knof, J., & Eichler, J. 1977 *Z. Physik* B **28**, 297.

DiDomenico, M. & Wemple, S.H.J. 1969 *J. Appl. Phys.* **40**, 720.

Flytzanis, C. 1969 *Phys. Rev. Lett.* **23**, 1336.

Flytzanis, C. 1971 *Phys. Lett.* A **34**, 99.

Fowler, P.W. & Madden, P.A. 1984 *Phys. Rev.* B **30**, 6131.

Fukunishi, S., Uchida, N., Miyazawa, S., & Noda, J. 1974 *Appl. Phys. Lett.* **24**, 424.

Gibbs, J.W. 1882 *Am. J. Sci.* **23**, 460.

Górski, P. & Kucharczyk, W. 1987 *Phys. Stat. Sol. (a)* **103**, K65.

Górski, P. & Kucharczyk, W. 1990 *Phys. Stat. Sol. (a)* **121**, K243.

Górski, P., Mik, D., Kucharczyk, W., & Raab, R.E. 1994 *Physica B* **193**, 17.

Graham, C. & Raab, R.E. 1994 *J. Opt. Soc. Am.* A **11**. 2137.

Graham, E.B., Pierrus, J., & Raab, R.E. 1992 *J. Phys.* B **25**, 4673.

Graham, E.B. & Raab, R.E. 1983 *Proc. R. Soc. Lond.* A **390**, 73.

Graham, E.B. & Raab, R.E. 1990 *Proc. R. Soc. Lond.* A **430**, 593.

Grib, B.N., Kondilenko, I.I., & Korotkov, P.A. 1975 *Zh. Prikl. Spectrosk.* **23**, 804; 1975 *J. Appl. Spectrosc.* (English Transl.) **23**, 1449.

Hartree, D.R. 1952 *Numerical Analysis.* Oxford: Clarendon Press.

Haussühl, S. & Weber, H.J. 1977 *Z. Kristallogr.* **145**, 257.

Jamroz, W. & Karniewicz, J. 1979 *Opt. Quantum Electronics* **11**, 23.

Jamroz, W. & Karniewicz, J., & Stachowiak, J. 1979 *Kvantovaya Electronika* **6**, 1365.

Johnson, M.D., Subbaswamy, K.R., & Senatore, G. 1987 *Phys. Rev* B **36**, 9202.

Jones, R.C. 1948 *J. Opt. Soc. Am.* **38**, 671.

Kaminow, I.P. 1974 *An Introduction to Electromagnetic Devices.* New York: Academic Press.

Kaminow, I.P. & Johnston, W.D. 1967 *Phys. Rev.* **160**, 519.

Kaminow, I.P. & Johnston, W.D. 1969 *Phys. Rev.* **188**, 1209.

Kaminow, I.P. & Turner, E.H. 1966 *Proc. IEEE.* **54**, 1374.

Kelly, R.L. 1966 *Phys. Rev.* **151**, 721.

Kerr, J. 1875 *Phil. Mag.* **40**, 337.

Kobayashi, J., Tamada, M., Hosogaya, N., & Someya, T. 1988 *Ferroelectrics Lett.* **8**, 145.

Kucharczyk, W. 1987 *J. Phys.* C **20**, 1875.

Kucharczyk, W. 1992 *Physica B* **176**, 189.

Landolt-Börnstein 1979 *Numerical Data and Functional Relationships in Science and Technology.* New Series, Group III, vol. 11, Berlin: Springer.

Levenson, M.D. & Bloembergen, N. 1974 *Phys. Rev.* B **10**, 4447.

Levine, B.F. 1973a *J. Chem. Phys.* **59**, 1463.

Levine, B.F. 1973b *Phys. Rev.* B **7**, 2600.

Lomova, L.G. & Sonin, A.S. 1968 *Fiz. Tverd. Tela.* **10**, 1565.

Maldonado, T.A. & Gaylord, T.K. 1988 *Appl. Optics* **27**, 5051.

Nakano, H. & Kimura, H. 1969 *J. Phys. Soc. Jpn.* **27**, 519.

Nakano, J., Shiozaki, Y., & Nakamura, F. 1973 *J. Phys. Soc. Jpn.* **34**, 1423.

Nelson, D.F. 1975 *J. Opt. Soc. Am.* **65**, 1144.

Nye, J.F. 1985 *Physical Properties of Crystals.* Oxford: Clarendon Press.

Onuki, K., Uchida, N., & Saku, T. 1972 *J. Opt. Soc. Am.* **62**, 1030.

Penn, D.R. 1962 *Phys. Rev.* **128**, 2093.

Perfilova, V.E. & Sonin, A.S. 1967 *Izv. Akad. Nauk. SSSR Ser. Fiz.* **31**, 1136; 1967 *Bull. Acad. Sci. USSR Phys. Ser.* (English Transl.) **31**, 1154.

Phillips, J.C. & Van Vechten, J.A. 1969 *Phys. Rev. Lett.* **22**, 705.

Pockels, F. 1906 *Lehrbuck der Kristalloptik.* Liepzig: Teubner.

Raab, R.E 1975 *Molec. Phys.* **29**, 1323.

Shih, C. & Yariv, A. 1980 *Phys. Rev. Lett.* **44**, 281.

Shih, C. & Yariv, A. 1982 *J. Phys.* C **15**, 825.

Troussant, F., Bastie, P., & Vallase, M. 1988 *Ferroelectrics* **88**, 45.

van Staden, E.M. 1993 MSc dissertation University of Natal, Pietermaritzburg.

Weisskopf, V. & Wigner, E. 1930 *Z. Phsc.* **63**, 54; **65**, 18.

Yariv, A. & Yeh, P. 1984 *Optical Waves in Crystals.* New York: John Wiley & Sons.

Zook, J.D., Chen, D., & Otto, G.N. 1967 *Appl. Phys. Lett.* **11**, 159.